General theory of intraband relaxation processes in heavily doped graphene

Kupčić, Ivan

General theory of intraband relaxation processes in heavily doped graphene

I. Kupčić[*]

Department of Physics, Faculty of Science, University of Zagreb, P.O. Box 331, HR-10002 Zagreb, Croatia
(Received 20 February 2015; revised manuscript received 16 April 2015; published 20 May 2015)

The frequency and wave-vector-dependent memory function in the longitudinal conductivity tensor of weakly interacting electronic systems is calculated by using an approach based on quantum transport equations. In this paper, we show that there is a close relation between the single-electron self-energy, the electron-hole pair self-energy, and the memory function. It is also shown in which way singular long-range Coulomb interactions, together with other $\mathbf{q} \approx \mathbf{0}$ scattering processes, drop out of both the memory function and the related transport equations. The theory is illustrated on heavily doped graphene, which is the prototype of weakly interacting single-band electron-phonon systems. A steplike increase of the width of the quasiparticle peak in angle-resolved photoemission spectra at frequencies of the order of the frequency of in-plane optical phonons is shown to be consistent with the behavior of an intraband plasmon peak in the energy loss spectroscopy spectra. Both anomalies can be understood as a direct consequence of weak electron scattering from in-plane optical phonons.

I. INTRODUCTION

The principal objective of this paper is to give an analytical background for accounting for intraband relaxation processes in weakly interacting electron-phonon systems. The formulas presented here can be used in comparative studies of transport [1,2], reflectivity [3], angle-resolved photoemission spectroscopy (ARPES) [4,5], and energy loss spectroscopy [6,7] data measured on doped graphene samples for $\hbar\omega < E_F$ and for a large enough Fermi energy E_F. Equally important, the present analysis can be easily extended to the interband conductivity and the interband relaxation processes in the intraband channel as well, which are both of importance in the study of the ballistic conductivity in graphene [1,2,8,9]. The numerical results regarding some of these issues will be given in a separate presentation [10]. Here, we only report on the results that illustrate the simplest effect, namely, the development of the single-electron spectral function and the energy loss function with wave vector for $\hbar\omega \approx \hbar\omega_{v\mathbf{q}'}$. The purpose of this part of the analysis is to justify in single-band electronic systems the use of the memory function in the analysis of the scattering by those boson modes whose properties are similar to those of in-plane optical phonons in graphene. The scattering by magnons in underdoped cuprate superconductors is one important example [11].

According to Ref. [12], we can use the Ward identity to show the dynamical conductivity of a general multiband electronic model in terms of the elements of the random phase approximation (RPA) irreducible response tensor $\pi_{\mu\nu}(\mathbf{q},\omega)$ ($\mu,\nu = 0,x,y,z$ in a general three-dimensional case, and $\mu,\nu = 0,x,y$ in graphene) and the total effective number of charge carriers $n_{\alpha\alpha}(\mathbf{q})$ in the following way:

$$\sigma_{\alpha\alpha}(\mathbf{q},\omega) = \frac{i}{q_\alpha}\pi_{\alpha 0}(\mathbf{q},\omega) = \frac{i}{\omega}\left(\pi_{\alpha\alpha}(\mathbf{q},\omega) + \frac{e^2 n_{\alpha\alpha}(\mathbf{q})}{m}\right) \quad (1)$$

[here $\mathbf{q} = q_\alpha \hat{e}_\alpha$ and $\alpha = x,y$ ($\alpha = x,y,z$) in two-dimensional (three-dimensional) systems]. The first expression will be referred to as the first Kubo formula for the conductivity

tensor, and the second one as the second Kubo formula [13]. The advantages of using the second Kubo formula have been discussed in detail in Mahan's textbook within a simple single-band model with the scattering from impurities, including the detailed examination of vertex effects [14]. The appearance of the product of two single-electron spectral functions of the same wave vector is an important characteristic of this approach, as well as the fact that it deals exclusively with the real part of $\sigma_{\alpha\alpha}(\mathbf{q},\omega)$ at $\mathbf{q} = \mathbf{0}$. The same approach has been frequently used in examinations of electrodynamic properties of low-dimensional strongly correlated electronic systems [15] as well as of doped graphene [16,17], usually with vertex effects neglected from the outset.

In this paper, we shall use the first Kubo formula with the vertex corrections taken into account to determine the dynamical conductivity of a general single-band model with all relevant retarded and nonretarded interactions included. This approach is based on the finite-temperature quantum transport equation derived from the Bethe-Salpeter equation for the intraband electron-hole propagators [18]. The most important fact about this approach is that the current-charge correlation function $\pi_{\alpha 0}(\mathbf{q},\omega)$ is expressed in terms of two different damping functions (the imaginary parts of the single-electron self-energy and of the electron-hole self-energy), and that it is a linear function of the single-electron spectral function $\mathcal{A}(\mathbf{k},\varepsilon)$. It will be shown below that this approach provides a unified diagrammatic representation for different multicomponent excitations in the electron-phonon system under consideration in which the forward scattering contributions and the normal and umklapp backward scattering contributions are distinctly resolved. Another advantage of the present approach over the second Kubo formula is that it can also be used to determine the structure of other correlation functions of interest, such as the self-energy of acoustic and optical phonons, as well as the structure of $\sigma_{\alpha\alpha}(\mathbf{q},\omega)$ at finite $\mathbf{q}$. In this way, it is possible to study in detail a rich variety of phenomena characterizing the case in which the energy of external electromagnetic fields $\hbar\omega$, the energy of in-plane optical phonons $\hbar\omega_{v\mathbf{q}'}$, and the energy of intraband plasmons $\hbar\omega_{\mathrm{pl}}(\mathbf{q})$ are comparable to each other [19–22].

_____
[*]Corresponding author: kupcic@phy.hr

It is shown here that, in the case where the dependence of the electron-phonon coupling function on wave vectors is negligible, the electron-electromagnetic field vertex corrections associated with electron scattering by optical phonons can be neglected. On the other hand, electron scattering by intraband plasmon modes produces dramatic changes in the single-electron self-energy (and in ARPES spectra) with respect to the self-energy of an electron-hole pair (which is relevant to both the dynamical conductivity and the energy loss function). Although the electrodynamic properties of heavily doped graphene are very similar to that of common metallic systems with parabolic dispersion, the single-electron spectral function of these two systems can be quite different, depending on the wave-vector dependence of both $\omega_{\mathrm{pl}}(\mathbf{q})$ and the electron-plasmon coupling function.

In Sec. II, we introduce the notation for bare and renormalized interactions in heavily doped graphene. The effects of the electron scattering by in-plane optical phonons on the single-electron spectral function are discussed in Sec. III. In Sec. IV, the first Kubo formula for the dynamical conductivity and the general soluon of the Bethe-Salpeter equation for the auxiliary electron-hole propagators are combined to determine the structure of the longitudinal dynamical conductivity in a general single-band case. In Sec. V, the spectral representation of the dynamical conductivity is shown for the case of weak electron-phonon interactions. Local charge conservation and gauge invariance of the present response theory are briefly discussed in Secs. V–VII. The effects of the scattering by in-plane optical phonons on the real part of the dynamical conductivity and on the energy loss function in doped graphene are studied in Sec. VIII. Section IX contains concluding remarks.

II. HEAVILY DOPED GRAPHENE

In doped graphene with the Fermi energy E_{F} large enough, low-energy electrodynamic properties are completely described in terms of the intraband contributions. The term low-energy is related here to the energy region $\hbar\omega < 0.8|E_{\mathrm{F}}|$, where the dynamical interband screening of the intraband plasmon modes is found to be negligible [12,23]. In this case, we restrict our attention to the intraband contribution to the conductivity tensor (1) and drop reference to the band index in all elements in this tensor as well as in the total Hamiltonian. The bare electronic Hamiltonian is thus given by

$$H_0^{\mathrm{el}} = \sum_{\mathbf{k}\sigma}[\varepsilon_0(\mathbf{k}) + \mu]c_{\mathbf{k}\sigma}^{\dagger}c_{\mathbf{k}\sigma}. \tag{2}$$

In the nearest-neighbor tight-binding approximation for conduction electrons, the bare electron dispersion in graphene, measured with respect to the chemical potential μ, is $\varepsilon_0(\mathbf{k}) = \varepsilon_{\pi}^0(\mathbf{k}) = -|t(\mathbf{k})| - \mu$, in the hole-doped case, and $\varepsilon_0(\mathbf{k}) = \varepsilon_{\pi^*}^0(\mathbf{k}) = |t(\mathbf{k})| - \mu$, in the electron-doped case [9,24] [$|t(\mathbf{k})|$ is given by Eq. (A7)]. The scattering Hamiltonian is the sum of two contributions, $H' = H_1' + H_2'$, where

$$H_1' = \sum_{\nu\mathbf{q}}\sum_{\mathbf{k}\sigma}\frac{G_{\nu}(\mathbf{k}_+,\mathbf{k})}{\sqrt{N}}(b_{\nu\mathbf{q}} + b_{\nu-\mathbf{q}}^{\dagger})c_{\mathbf{k}+\mathbf{q}\sigma}^{\dagger}c_{\mathbf{k}\sigma} \tag{3}$$

and

$$H_2' = \frac{1}{2}\sum_{\mathbf{k}\mathbf{k}'\mathbf{q}}\sum_{\sigma\sigma'}\frac{\varphi(\mathbf{q})}{V}c_{\mathbf{k}+\mathbf{q}\sigma}^{\dagger}c_{\mathbf{k}'\sigma'}^{\dagger}c_{\mathbf{k}'+\mathbf{q}\sigma'}c_{\mathbf{k}\sigma} \tag{4}$$

describe, respectively, all retarded and all nonretarded electron-electron interactions [12], with $\mathbf{k}_+ = \mathbf{k} + \mathbf{q}$.

In the finite-temperature formalism, it is customary to use the notation

$$W(\mathbf{k}_+,\mathbf{k}',\mathbf{k}_+',\mathbf{k},iv_m) = \frac{\varphi(\mathbf{q}')}{V} + \mathcal{F}(\mathbf{k}_+,\mathbf{k}',\mathbf{k}_+',\mathbf{k},iv_m) \tag{5}$$

for the renormalized two-point interaction and $U(\mathbf{k}_+,\mathbf{k}',\mathbf{k}_+',\mathbf{k},i\omega_{n+},i\omega_m,i\omega_{m+},i\omega_n)$ for the completely irreducible four-point interaction [14,25–27]. The retarded part of $W(\mathbf{k}_+,\mathbf{k}',\mathbf{k}_+',\mathbf{k},iv_m)$ is labeled by $\mathcal{F}(\mathbf{k}_+,\mathbf{k}',\mathbf{k}_+',\mathbf{k},iv_m)$. Here and hereafter, $i\omega_{n+} = i\omega_n + iv_n$, $\mathbf{q}' = \mathbf{k}' - \mathbf{k}$, and $iv_m = i\omega_m - i\omega_n$. Similarly, we separate from the completely irreducible four-point interaction $U(\mathbf{k}_+,\mathbf{k}',\mathbf{k}_+',\mathbf{k},i\omega_{n+},i\omega_m, i\omega_{m+},i\omega_n)$ two contributions. The first one describes the bare nonretarded contribution $\varphi(\mathbf{q}')/V$ and the second one, $\Delta U(\mathbf{k}_+,\mathbf{k}',\mathbf{k}_+',\mathbf{k},i\omega_{n+},i\omega_m,i\omega_{m+},i\omega_n)$, all other contributions. We also introduce the abbreviations for the renormalized interactions with two independent wave vectors; for example, $W(\mathbf{k},\mathbf{k}',iv_m) = \varphi(\mathbf{q}')/V + \mathcal{F}(\mathbf{k},\mathbf{k}',iv_m)$ is the abbreviation for $W(\mathbf{k},\mathbf{k}',\mathbf{k}',\mathbf{k},iv_m)$.

III. SINGLE-ELECTRON DYSON EQUATION

The Dyson equation for the single-electron Green's function is of the form

$$[i\hbar\omega_n - \varepsilon_0(\mathbf{k}) - \hbar\Sigma(\mathbf{k},i\omega_n)]\mathcal{G}(\mathbf{k},i\omega_n) = \hbar. \tag{6}$$

The same relation holds for the auxiliary Green's function $\widetilde{\mathcal{G}}(\mathbf{k},i\omega_n)$ (to be defined later). Here,

$$\hbar\Sigma(\mathbf{k},i\omega_n) = -\sum_{\mathbf{k}'\sigma'}\frac{1}{\beta\hbar}\sum_{i\omega_m}\mathcal{G}(\mathbf{k}',i\omega_m)U(\mathbf{k},\mathbf{k}',i\omega_n,i\omega_m) \tag{7}$$

is the single-electron self-energy and $U(\mathbf{k},\mathbf{k}',i\omega_n,i\omega_m)$ is the simplified version of the completely irreducible four-point interaction $U(\mathbf{k}_+,\mathbf{k}',\mathbf{k}_+',\mathbf{k},i\omega_{n+},i\omega_m,i\omega_{m+},i\omega_n)$. The skeleton series of diagrams from Fig. 1 represents the simplest form of $\Sigma(\mathbf{k},i\omega_n)$, which is expressed in terms of $\mathcal{G}(\mathbf{k},i\omega_n)$ and $W(\mathbf{k}_+,\mathbf{k}',\mathbf{k}_+',\mathbf{k},iv_m)$, rather than in terms of their bare forms. Such a structure of $\Sigma(\mathbf{k},i\omega_n)$ is an important assumption of

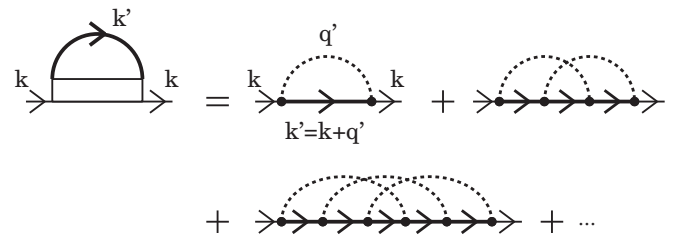
FIG. 1. The skeleton series for the single-electron self-energy $\Sigma(\mathbf{k},i\omega_n)$. $U(\mathbf{k},\mathbf{k}',i\omega_n,i\omega_m)$ (white rectangle) and $W(\mathbf{k},\mathbf{k}',iv_m) = \varphi(\mathbf{q}')/V + \mathcal{F}(\mathbf{k},\mathbf{k}',iv_m)$ (bold dashed line) are the completely irreducible four-point interaction and the renormalized two-point interaction.

the present self-consistent treatment of the single-electron and electron-hole propagators.

It is not hard to verify that two Dyson equations for $\mathcal{G}(\mathbf{k},i\omega_n)$ and $\mathcal{G}(\mathbf{k}_+,i\omega_{n+})$ can be combined to give

$$\mathcal{G}(\mathbf{k},i\omega_n)\mathcal{G}(\mathbf{k}_+,i\omega_{n+})$$
$$= \frac{\mathcal{G}(\mathbf{k},i\omega_n) - \mathcal{G}(\mathbf{k}_+,i\omega_{n+})}{i\nu_n + \varepsilon_0(\mathbf{k},\mathbf{k}_+)/\hbar + \Pi^0(\mathbf{k},\mathbf{k}_+,i\omega_n,i\omega_{n+})}, \quad (8)$$

where $\Pi^0(\mathbf{k},\mathbf{k}_+,i\omega_n,i\omega_{n+}) \equiv \Pi^0(\mathbf{k},\mathbf{q},i\nu_n,i\omega_n) = \Sigma(\mathbf{k},i\omega_n) - \Sigma(\mathbf{k}_+,i\omega_{n+})$ is the bare electron-hole self-energy and $\varepsilon_0(\mathbf{k},\mathbf{k}_+) = \varepsilon_0(\mathbf{k}) - \varepsilon_0(\mathbf{k}_+)$. The relation (8) is the basic relation that connects the Bethe-Salpeter equations with the quantum transport equations (see Sec. IV) [18,28].

A. *GW* approximation

In weakly interacting systems with the interactions independent of spin, we can make a simplification by replacing $U(\mathbf{k},\mathbf{k}',i\omega_n,i\omega_m)$ in Eq. (7) with the renormalized two-point interaction $W(\mathbf{k},\mathbf{k}',i\nu_m) = \varphi(\mathbf{q}')/V + \mathcal{F}(\mathbf{k},\mathbf{k}',i\nu_m)$ and using a similar approximation for $U(\mathbf{k}_+,\mathbf{k}',\mathbf{k}'_+,\mathbf{k},i\omega_{n+},i\omega_m,i\omega_{m+},i\omega_n)$ in Bethe-Salpeter equations. This approximation (corresponding to the first diagram in Fig. 1) can be understood as the effective Hartree-Fock approximation for $\Sigma(\mathbf{k},i\omega_n)$ [29] in which the bare retarded interaction $\mathcal{F}^0(\mathbf{k},\mathbf{k}',i\nu_m)$ is replaced by $\mathcal{F}(\mathbf{k},\mathbf{k}',i\nu_m)$. It is usually called the *GW* approximation.

In the general case described by Eqs. (3) and (4), the retarded part of $W(\mathbf{k},\mathbf{k}',i\nu_m)$ can be shown in the form

$$\mathcal{F}(\mathbf{k},\mathbf{k}',i\nu_m) = \sum_\nu \frac{|G_\nu(\mathbf{k},\mathbf{k}')|^2}{N\hbar}\mathcal{D}_\nu(\mathbf{q}',i\nu_m) + \frac{1}{V}\Delta\widetilde{\varphi}(\mathbf{q}',i\nu_m). \quad (9)$$

Here, $\mathcal{D}_\nu(\mathbf{q}',i\nu_m)$ is the phonon Green's function and $\Delta\widetilde{\varphi}(\mathbf{q}',i\nu_m) = \varphi(\mathbf{q}')/\varepsilon(\mathbf{q}',i\nu_m) - \varphi(\mathbf{q}')$ is the frequency-dependent part of the screened nonretarded interaction. The latter is equal to the screened dielectric susceptibility, $\widetilde{\chi}(\mathbf{q}',i\nu_m)$, multiplied by $|\varphi(\mathbf{q}')|^2$.

The interaction $U(\mathbf{k},\mathbf{k}',i\omega_n,i\omega_m)$ produces two qualitatively different effects in the single-electron self-energy (7),

$$\hbar\Sigma(\mathbf{k},i\omega_n) = \Delta\tilde{\varepsilon}^{\mathrm{HF}}(\mathbf{k}) + \hbar\Delta\Sigma(\mathbf{k},i\omega_n). \quad (10)$$

The interaction $\varphi(\mathbf{q}')$ gives the well-known purely real Hartree-Fock correction to the electron dispersion, $\Delta\tilde{\varepsilon}^{\mathrm{HF}}(\mathbf{k})$, which is usually added to the bare electron dispersion $\varepsilon_0(\mathbf{k})$ to give $\tilde{\varepsilon}(\mathbf{k}) = \varepsilon_0(\mathbf{k}) + \Delta\tilde{\varepsilon}^{\mathrm{HF}}(\mathbf{k})$. On the other hand, $\Delta U(\mathbf{k},\mathbf{k}',i\omega_n,i\omega_m)$ in $\Delta\Sigma(\mathbf{k},i\omega_n)$ leads to various types of damping effects and, through the Kramers-Kronig relations, to additional corrections to the electron dispersion. For example, the scattering of conduction electrons by phonon modes leads to [14]

$$\hbar\Delta\Sigma(\mathbf{k},\omega) = \frac{1}{N}\sum_{\nu\mathbf{k}'}|G_\nu(\mathbf{k},\mathbf{k}')|^2 \int_{-\infty}^\infty \frac{d\varepsilon'}{2\pi}\int_{-\infty}^\infty \frac{d\omega'}{2\pi}\mathcal{A}(\mathbf{k}',\varepsilon')$$
$$\times \mathcal{B}_\nu(\mathbf{k}'-\mathbf{k},\omega')\frac{f^b(\omega') + f(\varepsilon')}{\hbar\omega + i\eta - \varepsilon' + \hbar\omega'}. \quad (11)$$

Here, $f^b(\omega)$ is the Bose-Einstein distribution function, $f(\varepsilon)$ is the Fermi-Dirac distribution function [with $f(-\varepsilon) = 1 -$

$f(\varepsilon)$], $\mathcal{A}(\mathbf{k},\varepsilon)$ is the single-electron spectral function introduced by

$$\mathcal{G}(\mathbf{k},i\omega_n) = \int_{-\infty}^\infty \frac{d\varepsilon}{2\pi}\frac{\mathcal{A}(\mathbf{k},\varepsilon)}{i\omega_n - \varepsilon/\hbar}, \quad (12)$$

and $\mathcal{B}_\nu(\mathbf{q}',\omega')$ is the boson spectral function defined by

$$\mathcal{D}_\nu(\mathbf{q}',i\nu_m) = \int_{-\infty}^\infty \frac{d\omega'}{2\pi}\frac{\mathcal{B}_\nu(\mathbf{q}',\omega')}{i\nu_m - \omega'}. \quad (13)$$

B. Second-order perturbation theory

The result of the direct diagrammatic calculation of the $(H_1')^2$ contributions to $\Sigma(\mathbf{k},\omega)$ is [14,29]

$$\hbar\Sigma^{[2]}(\mathbf{k},\omega) \equiv \hbar\Sigma^{[2]}(\mathbf{k},\omega + i\eta)$$
$$= \frac{1}{N}\sum_{\nu\mathbf{k}'}|G_\nu(\mathbf{k},\mathbf{k}')|^2$$
$$\times \sum_{s=\pm 1}\frac{f^b(\omega_{\nu\mathbf{k}'-\mathbf{k}}) + f(s\varepsilon(\mathbf{k}'))}{\hbar\omega + i\eta - \varepsilon(\mathbf{k}') + s\hbar\omega_{\nu\mathbf{k}'-\mathbf{k}}}. \quad (14)$$

This result can also be obtained by substituting

$$\mathcal{A}(\mathbf{k},\varepsilon) \approx \mathcal{A}^0(\mathbf{k},\varepsilon) = 2\pi\delta(\varepsilon - \varepsilon(\mathbf{k})),$$
$$\mathcal{B}_\nu(\mathbf{q}',\omega') \approx \mathcal{B}_\nu^0(\mathbf{q}',\omega') = 2\pi\sum_{s=\pm 1}s\delta(\omega' - s\omega_{\nu\mathbf{q}'}) \quad (15)$$

into Eq. (11) and using the relation $s[f^b(s\omega_{\nu\mathbf{k}'-\mathbf{k}}) + f(\varepsilon(\mathbf{k}'))] = f^b(\omega_{\nu\mathbf{k}'-\mathbf{k}}) + f(s\varepsilon(\mathbf{k}'))$.

For $H' = H_2'$, low-order perturbation theory for $\Delta\Sigma(\mathbf{k},\omega)$ starts with the $(H_2')^2$ contributions. The leading term is described by the first diagram in Fig. 1 as well, with $[|G_\nu(\mathbf{k},\mathbf{k}')|^2/N\hbar]\mathcal{D}_\nu(\mathbf{q}',\omega)$ replaced by $[|\varphi(\mathbf{q}')|^2/V]\widetilde{\chi}(\mathbf{q}',\omega)$. The result is

$$\hbar\Sigma^{[4]}(\mathbf{k},\omega) = \sum_{\mathbf{k}'\mathbf{q}}\frac{|\varphi(\mathbf{q})|^2}{V^2}[f(\mathbf{k}') - f(\mathbf{k}'_+)]$$
$$\times \frac{f^b(\omega(\mathbf{k}'_+,\mathbf{k}')) + f(\mathbf{k}_+)}{\hbar\omega + i\eta - \varepsilon(\mathbf{k}_+) + \varepsilon(\mathbf{k}'_+,\mathbf{k}')}, \quad (16)$$

with $\varepsilon(\mathbf{k},\mathbf{k}') = \varepsilon(\mathbf{k}) - \varepsilon(\mathbf{k}') \equiv \hbar\omega(\mathbf{k},\mathbf{k}')$ and $f(\varepsilon(\mathbf{k})) \equiv f(\mathbf{k})$.

C. Electron-phonon coupling in graphene

When considering the scattering of conduction electrons by in-plane optical phonons in graphene, we can simplify the expression (14) by $\omega_{\nu\mathbf{q}'} \approx \omega_{\mathrm{LO}\mathbf{q}'} \approx \omega_{\mathrm{op}}$, $g_\nu^2/M_\nu \approx g_{\mathrm{LO}}^2/M_{\mathrm{LO}}$, and $\eta \to \hbar\Sigma^i$. Here, the phenomenological damping energy $\hbar\Sigma^i$ mimics the finite width of $\mathcal{A}(\mathbf{k}',\varepsilon')$ in Eq. (11) as well as the effects of the electron-phonon vertex corrections not included in Eq. (11). Although this approximation is similar to the relaxation-time approximation, which is widely used in the study of the dynamical conductivity of weakly interacting systems, it is easily seen that the energy $2\hbar\Sigma^i$ is actually well above the energy $\hbar/\tau_{\mathrm{tr}}$ (τ_{tr} is the transport relaxation time). The reasons for that are explained below.

In graphene, the dependence of the intraband coupling between conduction electrons and in-plane optical phonons in Eq. (14) on wave vectors can be neglected [16]. For E_F not

too large, we can write (see Appendix A)

$$|G_\nu(\mathbf{k}',\mathbf{k})|^2 \approx \frac{1}{2}\sum_{\nu(op)}|G_\nu(\mathbf{k}',\mathbf{k})|^2$$

$$\approx \frac{\hbar g_{LO}^2}{4M_{LO}\omega_{LO\mathbf{k}'-\mathbf{k}}}\sum_{\nu(op)}\left|q_\nu^{ss}(\mathbf{k}',\mathbf{k})\right|^2 \quad (17)$$

and then use the Dirac cone approximation for $q_\nu^{ss}(\mathbf{k}',\mathbf{k})$ [12],

$$\left|q_\alpha^{ss}(\mathbf{k}',\mathbf{k})\right|^2 \approx \left|q_\alpha^{ss}(\mathbf{k})\right|^2 \approx (3\tilde{k}_\alpha/\tilde{k})^2, \quad (18)$$

to obtain

$$|G_\nu(\mathbf{k}',\mathbf{k})|^2 \approx |G_\nu|^2 \approx \frac{\hbar(9g_{LO}^2/2)}{2M_{LO}\omega_{LO\mathbf{0}}}. \quad (19)$$

D. ARPES spectral functions

In order to determine the structure of the single-electron spectral function

$$\mathcal{A}(\mathbf{k},\varepsilon) = \frac{-2\hbar\Sigma^i(\mathbf{k},\omega)}{[\hbar\omega - E(\mathbf{k},\omega)]^2 + [\hbar\Sigma^i(\mathbf{k},\omega)]^2} \quad (20)$$

at energies $|\varepsilon| \equiv |\hbar\omega| \approx \hbar\omega_{LO\mathbf{q}'}$, it is convenient to show the single-electron self-energy $\Sigma(\mathbf{k},\omega) = \Sigma^r(\mathbf{k},\omega) + i\Sigma^i(\mathbf{k},\omega)$ as a sum of two contributions, $\Sigma(\mathbf{k},\omega) = \Sigma_{op}(\mathbf{k},\omega) + \delta\Sigma(\mathbf{k},\omega)$ [as usual, $E(\mathbf{k},\omega) = \varepsilon_0(\mathbf{k}) + \hbar\Sigma^r(\mathbf{k},\omega)$, with $\mu \approx E_F$ hereafter]. In numerical calculations, the scattering from in-plane optical phonons is described by Eq. (14), in which the sum $\sum_{\nu(op)}$ runs over two in-plane optical phonon branches, resulting in $\Sigma_{op}(\mathbf{k},\omega)$. The damping energy $\hbar\delta\Sigma^i(\mathbf{k},\omega)$, associated with other scattering channels, is assumed to be of the form $a + |\hbar\omega|b$, where a and b are two adjustable parameters. $|G_{op}|^2 = \sum_{\nu(op)}|G_\nu|^2$ from Eq. (19) is another adjustable parameter in the spectral function (20). $\delta\Sigma^r(\mathbf{k},\omega)$ is neglected in the present considerations.

Figure 2 shows the real and imaginary parts of $-\hbar\Sigma_{op}(\mathbf{k},\omega)$ obtained in this way for $\mathbf{k} = (k_x,0)$ and $k_x = 1.95\,\text{Å}^{-1}$. It must
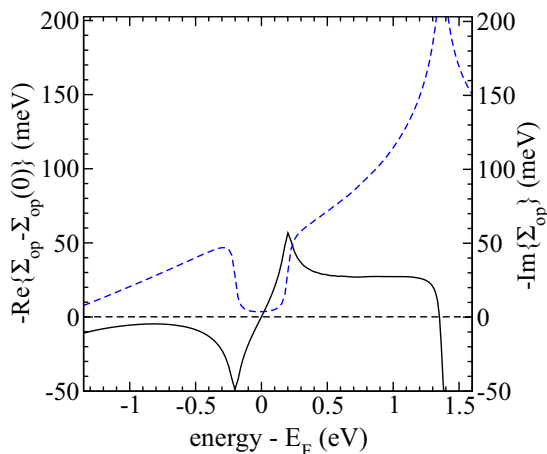
FIG. 2. (Color online) The real part (solid line) and the imaginary part (dashed line) of $-\hbar\Sigma_{op}(\mathbf{k},\omega)$ in the π^* band, for $\mathbf{k} = (k_x,0)$, $k_x = 1.95\,\text{Å}^{-1}$, $t = 2.52\,\text{eV}$, $E_F = 1.35\,\text{eV}$, $|G_{op}|^2 = 0.2\,\text{eV}^2$, $\hbar\omega_{op} = 0.2\,\text{eV}$, $\eta = \hbar\Sigma^i = 20\,\text{meV}$, and $T = 30\,\text{K}$. For these values of parameters, we obtain $-\text{Re}\{\hbar\Sigma_{op}(\mathbf{k},0)\} = 81.5\,\text{meV}$, which corresponds to the change of the chemical potential, $\delta\mu$.
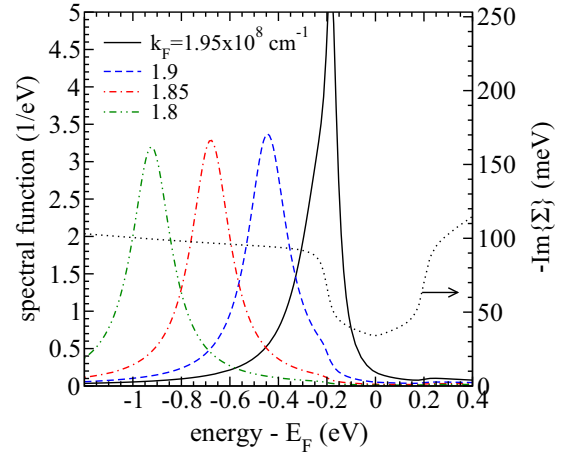
FIG. 3. (Color online) The spectral function $(1/2\pi)\mathcal{A}(\mathbf{k},\varepsilon)$ in the π^* band for $\mathbf{k} = (k_x,0)$, $k_x = 1.8, 1.85, 1.9$, and $1.95\,\text{Å}^{-1}$. Dotted line: the damping function $-\hbar\Sigma^i(\mathbf{k},\omega)$. The parameters are the same as in Fig. 2, with $\hbar\delta\Sigma^i(\mathbf{k},\omega) = a + |\hbar\omega|b$, and $a = 0.03\,\text{eV}$, $b = 0.05$.

be noticed that for $|G_\nu(\mathbf{k}',\mathbf{k})|^2 \approx |G_\nu|^2$ and $\hbar\omega_{\nu\mathbf{q}'} \approx \hbar\omega_{op}$, the function $-\Sigma_{op}^i(\mathbf{k},\omega)$ follows the density of states shifted roughly by $-\hbar\omega_{op}$ ($+\hbar\omega_{op}$) for $\varepsilon < 0$ ($\varepsilon > 0$). One important consequence of this observation is that particle-hole symmetry of $\Sigma(\mathbf{k},\omega)$ is broken in graphene [i.e., $\hbar\Sigma_{op}^i(\mathbf{k},\omega)$ is not an even function of ω]. This makes the Kramers-Kronig analysis of ARPES data measured in graphene more complicated than in usual weakly interacting systems. On the other hand, the memory-function $M_\alpha(\mathbf{k},\omega)$ from Sec. VIII has particle-hole symmetry by definition.

Experimental data measured in electron-doped graphene with $E_F \approx 1.35\,\text{eV}$ [5] are characterized by a steplike increase of $\Sigma^i(\mathbf{k},\omega)$ from the value $\approx 40\,\text{meV}$ below the threshold energy $|\varepsilon| = \hbar\omega_{LO\mathbf{q}'}$ to the value $\approx 80\,\text{meV}$ above this energy. To obtain the desired behavior of $-\Sigma^i(\mathbf{k},\omega)$ ($\approx$const) for $-E_F < \varepsilon < -\hbar\omega_{LO\mathbf{q}'}$, it is necessary to take into account frequency dependent contributions to $\hbar\delta\Sigma^i(\mathbf{k},\omega)$, which are associated with the scattering from other electrons. Similarly, in the energy region $-\hbar\omega_{LO\mathbf{q}'} < \varepsilon < 0$, the damping energy $-\hbar\Sigma^i(\mathbf{k},\omega)$ is predominantly related to the scattering from static disorder and from acoustic phonons [4]. The latter contribution is of relevance when considering the temperature effects in $\mathcal{A}(\mathbf{k},\varepsilon)$.

Figure 3 illustrates the dependence of the spectral function $(1/2\pi)\mathcal{A}(\mathbf{k},\varepsilon)$ on the wave vector in the vicinity of the K point, in the same case. The full width at half maximum is in agreement with experimental data from Ref. [5], confirming that $|G_{op}|^2 \approx 0.2\,\text{eV}^2$ and $\hbar\delta\Sigma^i(\omega) \approx a + |\hbar\omega|b$, with $a = 0.03\,\text{eV}$ and $b = 0.05$, in the leading approximation. This value of $|G_{op}|^2$ is also in agreement with the generally accepted value of the electron-phonon coupling constant g_{LO} [16].

E. Momentum distribution function

The momentum distribution function is an important ingredient of all response functions treated by means of the memory-function approximation. It is defined by $n(\mathbf{k}) = $

$(1/\beta\hbar)\sum_{i\omega_n}\mathcal{G}(\mathbf{k},i\omega_n)$, leading to

$$n(\mathbf{k}) = \int_{-\infty}^{\infty}\frac{d\varepsilon}{2\pi}\mathcal{A}(\mathbf{k},\varepsilon)f(\varepsilon). \tag{21}$$

For example, it helps us to incorporate the damping energy $\Sigma^i(\mathbf{k},\omega)$ from the single-electron spectral function $\mathcal{A}(\mathbf{k},\varepsilon)$ into the conductivity formulas (32) and (33).

IV. BETHE-SALPETER EQUATIONS

At finite temperatures, low-energy electrodynamic properties of heavily doped graphene can be described by the first Kubo formula for the intraband conductivity tensor ($\mathbf{q} = q_\alpha\hat{e}_\alpha$)

$$\sigma_{\alpha\alpha}(\mathbf{q},\tau) = \frac{i}{q_\alpha}\pi_{\alpha0}(\mathbf{q},\tau) \equiv \pi_{\alpha\bar{\alpha}}(\mathbf{q},\tau)$$

$$= \frac{1}{\hbar V}\langle T_\tau[\hat{J}_\alpha(\mathbf{q},\tau)\hat{P}_\alpha(-\mathbf{q},0)]\rangle_{\text{irred}}. \tag{22}$$

The two density operators in question are the intraband current density operator $\hat{J}_\alpha(\mathbf{q})$ and the intraband dipole density operator $-\hat{P}_\alpha(-\mathbf{q})$. Here, $J_\alpha(\mathbf{k},\mathbf{k}_+)$ and $J_{\bar{\alpha}}(\mathbf{k}_+,\mathbf{k}) \equiv -P_\alpha(\mathbf{k}_+,\mathbf{k}) = i\hbar J_\alpha(\mathbf{k}_+,\mathbf{k})/\varepsilon_0(\mathbf{k}_+,\mathbf{k}) \approx ie/q_\alpha$ are the corresponding bare vertex functions [12,18]. An alternative to the use of Eq. (22) is the second Kubo formula (35) in which $\sigma_{\alpha\alpha}(\mathbf{q},\tau)$ is expressed in terms of the current-current correlation function $\pi_{\alpha\alpha}(\mathbf{q},\tau)$. In both cases, we can write $\sigma_{\alpha\alpha}(\mathbf{q},\tau) \approx \sigma_{\alpha\alpha}^0(\mathbf{q},\tau)$, in the leading approximation. The bare conductivity tensor $\sigma_{\alpha\alpha}^0(\mathbf{q},i\nu_n)$ comprises by definition only the contributions that are irreducible with respect to both the long-range and short-range RPA interactions.

Any consistent study of the dynamical conductivity in doped graphene requires thus the understanding of the
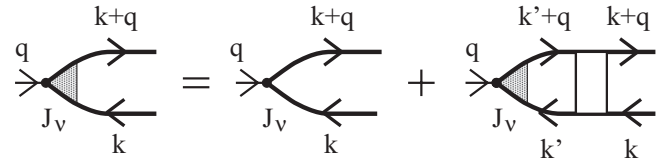

FIG. 4. The Bethe-Salpeter equation for the auxiliary electron-hole propagator $\Phi_\nu^0(\mathbf{k},\mathbf{k}_+,i\omega_n,i\omega_{n+})$. The white rectangle represents the irreducible four-point interaction $U^0(\mathbf{k}_+,\mathbf{k}',\mathbf{k}'_+,\mathbf{k},i\omega_{n+},i\omega_m,i\omega_{m+},i\omega_n)$.

elements of the RPA irreducible 4×4 response tensor $\pi_{\mu\nu}(\mathbf{q},i\nu_n)$ [30] and their bare forms,

$$\pi_{\mu\nu}^0(\mathbf{q},i\nu_n) = \frac{1}{V}\sum_{\mathbf{k}\sigma}J_\mu(\mathbf{k},\mathbf{k}_+)\frac{1}{\beta}\sum_{i\omega_n}\Phi_\nu^0(\mathbf{k},\mathbf{k}_+,i\omega_n,i\omega_{n+}), \tag{23}$$

where $\mu,\nu = 0,x,y$, and $J_0(\mathbf{k},\mathbf{k}_+) \approx e$ is the charge vertex function. The self-consistent Bethe-Salpeter equation for the auxiliary electron-hole propagator $\Phi_\nu^0(\mathbf{k},\mathbf{k}_+,i\omega_n,i\omega_{n+})$ is illustrated in Fig. 4. It has a simple self-consistent structure, but, by using Eq. (8), can be transformed into a much more transparent expression known as the quantum transport equation [18,28]. In order to make the analysis of this equation easier, we take into account the aforementioned nonretarded Hartree-Fock contributions and the corresponding vertex corrections by replacing the dispersion $\varepsilon_0(\mathbf{k})$ by $\varepsilon(\mathbf{k}) = \varepsilon_0(\mathbf{k}) + \Delta\varepsilon^{\text{HF}}(\mathbf{k})$ and by replacing the irreducible four-point interaction in which the long-range and short-range RPA contributions are disregarded, $U^0(\mathbf{k}_+,\mathbf{k}',\mathbf{k}'_+,\mathbf{k},i\omega_{n+},i\omega_m,i\omega_{m+},i\omega_n)$, by $\Delta U^0(\mathbf{k}_+,\mathbf{k}',\mathbf{k}'_+,\mathbf{k},i\omega_{n+},i\omega_m,i\omega_{m+},i\omega_n)$ [notice that $\varepsilon(\mathbf{k}) - \varepsilon(\mathbf{k}_+) \neq \tilde{\varepsilon}(\mathbf{k}) - \tilde{\varepsilon}(\mathbf{k}_+)$]. The result is

$$[i\hbar\nu_n + \varepsilon(\mathbf{k},\mathbf{k}_+)]\Phi_\nu^0(\mathbf{k},\mathbf{k}_+,i\omega_n,i\omega_{n+}) = \frac{1}{\hbar}[\mathcal{G}(\mathbf{k},i\omega_n) - \mathcal{G}(\mathbf{k}_+,i\omega_{n+})]J_\nu(\mathbf{k}_+,\mathbf{k}) - \lambda^2[\hbar\Delta\Sigma(\mathbf{k},i\omega_n) - \hbar\Delta\Sigma(\mathbf{k}_+,i\omega_{n+})]$$

$$\times \Phi_\nu^0(\mathbf{k},\mathbf{k}_+,i\omega_n,i\omega_{n+}) - \lambda^2\frac{1}{\hbar}[\mathcal{G}(\mathbf{k},i\omega_n) - \mathcal{G}(\mathbf{k}_+,i\omega_{n+})]\sum_{\mathbf{k}'\sigma'}\frac{1}{\beta}\sum_{i\omega_m}\Phi_\nu^0(\mathbf{k}',\mathbf{k}'_+,i\omega_m,i\omega_{m+})$$

$$\times \Delta U^0(\mathbf{k}_+,\mathbf{k}',\mathbf{k}'_+,\mathbf{k},i\omega_{n+},i\omega_m,i\omega_{m+},i\omega_n), \tag{24}$$

with the perturbation parameter λ^2 set to unity. The renormalized electron-hole pair energy in the abbreviated notation is $\varepsilon(\mathbf{k},\mathbf{k}_+) = \varepsilon(\mathbf{k}) - \varepsilon(\mathbf{k}_+)$. The relaxation processes are clearly distinguished here from the purely real Hartree-Fock corrections to $\varepsilon_0(\mathbf{k}) - \varepsilon_0(\mathbf{k}_+)$, $\Delta\varepsilon^{\text{HF}}(\mathbf{k}) - \Delta\varepsilon^{\text{HF}}(\mathbf{k}_+)$. The latter ones are unimportant when considering the Drude regime, corresponding to $\omega^2 \gg q_\alpha^2 v_\alpha^2(\mathbf{k})$, and, consequently, can be neglected hereafter. The discussion of the Thomas-Fermi regime $\omega^2 < q_\alpha^2 v_\alpha^2(\mathbf{k})$ is also interesting, but it is beyond the scope of the present analysis.

A. Formal solution

Since the last term on the right-hand side of Eq. (24) is an integral over all values of $\mathbf{k}'$ and $i\omega_m$, with the electron-hole propagator being a function of both $\mathbf{k}'$ and $i\omega_m$, this equation

is an integral equation of a complicated kind. The solution of this integral equation can be obtained by iteration and shown in powers of λ^2. Evidently, this method represents the high-energy expansion of the auxiliary electron-hole propagator $\Phi_\nu^0(\mathbf{k},\mathbf{k}_+,i\omega_n,i\omega_{n+})$ [31]. It is characterized by explicit control of the law of conservation of energy and momentum and by precise characterization of the elementary excitations in the electron-phonon system under consideration, in both Kubo formulas for the conductivity tensor.

There are three different ways to find the solution to this equation, which are associated with three conductivity formulas: the generalized Drude formula, the memory-function conductivity formula, and the electron-hole self-energy conductivity formula. Strictly speaking, they represent three different levels of the generalization of the ordinary Drude formula (51). For example, the electron-hole self-energy

conductivity formula is the generalization of the ordinary Drude formula to the case in which the relaxation function in question depends on both wave vectors and on both energy variables and where the single-electron spectral function has the finite width.

In these three approaches, the dynamical conductivity $\sigma_{\alpha\alpha}(\mathbf{q},\omega)$ is given in terms of $\pi_{\mu\nu}^{(2n)}(\mathbf{q},\omega)$, introduced by

$$\pi_{\mu\nu}(\mathbf{q},\omega) = \sum_{n=0}^{\infty} \lambda^{2n} \pi_{\mu\nu}^{(2n)}(\mathbf{q},\omega). \tag{25}$$

The latter correlation functions are obtained by analytical continuation of

$$\pi_{\mu\nu}(\mathbf{q},iv_n) \approx \pi_{\mu\nu}^0(\mathbf{q},iv_n)$$

$$= \frac{1}{V} \sum_{\mathbf{k}\sigma} J_\mu(\mathbf{k},\mathbf{k}_+) \frac{1}{\beta} \sum_{i\omega_n} \big[\Phi_\nu^{(0)}(\mathbf{k},\mathbf{k}_+,i\omega_n,i\omega_{n+})$$

$$+ \lambda^2 \Delta\Phi_\nu^{(2)}(\mathbf{k},\mathbf{k}_+,i\omega_n,i\omega_{n+}) + \cdots \big], \tag{26}$$

where

$$\Phi_\nu^{(0)}(\mathbf{k},\mathbf{k}_+,i\omega_n,i\omega_{n+}) = \frac{1}{i\hbar v_n + \varepsilon(\mathbf{k},\mathbf{k}_+)} \frac{1}{\hbar} [\mathcal{G}(\mathbf{k},i\omega_n)$$

$$- \mathcal{G}(\mathbf{k}_+,i\omega_{n+})] J_\nu(\mathbf{k}_+,\mathbf{k}), \tag{27}$$

and

$$\Delta\Phi_\nu^{(2)}(\mathbf{k},\mathbf{k}_+,i\omega_n,i\omega_{n+})$$

$$= -\Phi_\nu^{(0)}(\mathbf{k},\mathbf{k}_+,i\omega_n,i\omega_{n+}) \Bigg\{ \frac{1}{i\hbar v_n + \varepsilon(\mathbf{k},\mathbf{k}_+)}$$

$$\times [\hbar\Delta\Sigma(\mathbf{k},i\omega_n) - \hbar\Delta\Sigma(\mathbf{k}_+,i\omega_{n+})]$$

$$- \frac{1}{J_\nu(\mathbf{k}_+,\mathbf{k})} \sum_{\mathbf{k}'\sigma'} \frac{1}{\beta} \sum_{i\omega_m} \Phi_\nu^{(0)}(\mathbf{k}',\mathbf{k}'_+,i\omega_m,i\omega_{m+})$$

$$\times \Delta U^0(\mathbf{k}_+,\mathbf{k}',\mathbf{k}'_+,\mathbf{k},i\omega_{n+},i\omega_m,i\omega_{m+},i\omega_n) \Bigg\}. \tag{28}$$

The first term in Eq. (26) depends on the renormalized two-point interactions (5) only through two momentum distribution functions, while the second term includes the interactions from the scattering Hamiltonian $H' = H'_1 + H'_2$ through two self-energy contributions and the corresponding vertex corrections as well. In both of them, $i\hbar v_n + \varepsilon(\mathbf{k},\mathbf{k}_+)$ can be approximated by $i\hbar v_n$.

In the electron-hole self-energy approximation, we compare Eq. (26) with the λ^0 and λ^2 contributions to the formula

$$\pi_{\mu\nu}(\mathbf{q},iv_n)$$

$$= \frac{1}{V} \sum_{\mathbf{k}\sigma} J_\mu(\mathbf{k},\mathbf{k}_+) J_\nu(\mathbf{k}_+,\mathbf{k}) \frac{1}{\beta\hbar}$$

$$\times \sum_{i\omega_n} \frac{\mathcal{G}(\mathbf{k},i\omega_n) - \mathcal{G}(\mathbf{k}_+,i\omega_{n+})}{i\hbar v_n + \varepsilon(\mathbf{k},\mathbf{k}_+) + \lambda^2\hbar\Delta\Pi_{\mu\nu}(\mathbf{k},\mathbf{k}_+,i\omega_n,i\omega_{n+})} \tag{29}$$

to determine the structure of the complex relaxation function $\Delta\Pi_{\mu\nu}(\mathbf{k},\mathbf{k}_+,i\omega_n,i\omega_{n+}) \equiv \Delta\Pi_{\mu\nu}(\mathbf{k},\mathbf{q},iv_n,i\omega_n)$, here called the electron-hole self-energy.

This expression for the elements of the RPA irreducible 4×4 response tensor is the first important result of the present pa-

per. $\pi_{\mu\nu}(\mathbf{q},iv_n)$ is shown here, for the first time, in terms of the exact single-electron Green's function $\mathcal{G}(\mathbf{k},i\omega_n)$ and, in principle, the exact electron-hole self-energy $\Pi_{\mu\nu}(\mathbf{k},\mathbf{k}_+,i\omega_n,i\omega_{n+})$. The latter is defined implicitly by Eq. (28) and represents the general expression for the relaxation function attributed to the response function $\pi_{\mu\nu}(\mathbf{q},iv_n)$.

This expression for $\pi_{\mu\nu}(\mathbf{q},iv_n)$ has a wide range of applicability. For example, it can be used to determine the gauge-invariant structure of the intraband conductivity tensor in different strongly interacting systems (the cuprate superconductors being an example), or to reconsider open questions regarding electrodynamic properties of graphene. In most of these cases, it is possible to simplify this quite general expression by replacing the relaxation function $\Pi_{\mu\nu}(\mathbf{k},\mathbf{k}_+,i\omega_n,i\omega_{n+})$ by the quantity usually called the memory function. In the transport regime of common metallic systems, the quantum transport equation (24) reduces to the ordinary transport equation and the latter relaxation function reduces to the wave-vector dependent relaxation rate [32,33].

In order to illustrate the standard methods of calculating $\pi_{\mu\nu}(\mathbf{q},iv_n)$ in simple metallic systems in a way which preserves gauge invariance of the response functions (29), we shall consider first the case of weak electron-phonon coupling (Sec. V) and then apply the results to heavily doped graphene (Sec. VIII). Before doing this, let us emphasize some general properties of the response functions (29).

B. Direct versus indirect contributions

The factor $\mathcal{G}(\mathbf{k},i\omega_n) - \mathcal{G}(\mathbf{k}_+,i\omega_{n+})$ in Eq. (29) can be shown in the following way [34]:

$$\mathcal{G}(\mathbf{k},i\omega_n) - \mathcal{G}(\mathbf{k}_+,i\omega_{n+}) = [\mathcal{G}(\mathbf{k},i\omega_{n+}) - \mathcal{G}(\mathbf{k}_+,i\omega_{n+})]$$

$$+ [\mathcal{G}(\mathbf{k},i\omega_n) - \mathcal{G}(\mathbf{k},i\omega_{n+})]. \tag{30}$$

The contributions to $\pi_{\mu\nu}(\mathbf{q},iv_n)$ originating, respectively, from the first and the second term in this expression will be referred to as the direct and indirect contributions. There is a well-defined exclusion rule here which has been overlooked in the literature. The direct contributions are relevant only to the correlation functions (29) in which at least one vertex is the monopole-charge vertex. Their contribution to the current-current correlation function $\pi_{\alpha\alpha}(\mathbf{q},iv_n)$ is thus negligible, due to the factor q_α^2. In $\pi_{\alpha\alpha}(\mathbf{q},iv_n)$, the leading role is played by the indirect contributions.

C. Conductivity tensor

Let us now focus our attention to the direct contributions to the current-dipole correlation function $\pi_{\alpha\bar{\alpha}}(\mathbf{q},\omega)$. The corresponding conductivity tensor $\sigma_{\alpha\alpha}(\mathbf{q},\omega)$ is given by analytical continuation of

$$\sigma_{\alpha\alpha}(\mathbf{q},iv_n)$$

$$= \frac{1}{V} \sum_{\mathbf{k}\sigma} J_\alpha(\mathbf{k},\mathbf{k}_+) P_\alpha(\mathbf{k},\mathbf{k}_+) \frac{1}{\beta\hbar}$$

$$\times \sum_{i\omega_n} \frac{\mathcal{G}(\mathbf{k},i\omega_{n+}) - \mathcal{G}(\mathbf{k}_+,i\omega_{n+})}{i\hbar v_n + \varepsilon(\mathbf{k},\mathbf{k}_+) + \lambda^2\hbar\Delta\Pi(\mathbf{k},\mathbf{k}_+,i\omega_n,i\omega_{n+})}. \tag{31}$$

As shown below, we can use the spectral representation of the single-particle propagators to show Eq. (31) in two slightly different forms. The first one will be referred to as the Boltzmann representation of $\sigma_{\alpha\alpha}(\mathbf{q},\omega)$ and the second one as the Drude representation. They describe the low-energy physics of weakly interacting systems equally well. Notice also that the conductivity tensor (31) has the same form as the result of the averaging procedure used in Appendix B, Eqs. (B3) and (B4).

Similarly, summation over $i\omega_n$ in Eqs. (27) and (28) gives the result, which can be easily compared to the expansion of the memory-function conductivity formula

$$\sigma_{\alpha\alpha}(\mathbf{q},\omega) = \frac{1}{V}\sum_{\mathbf{k}\sigma}\frac{n(\mathbf{k})-n(\mathbf{k}_+)}{\varepsilon_0(\mathbf{k}_+)-\varepsilon_0(\mathbf{k})}\frac{i|J_\alpha(\mathbf{k},\mathbf{k}_+)|^2}{\omega+\lambda^2 M(\mathbf{k},\mathbf{q},\omega)}$$

$$\approx \frac{ie}{m}\frac{1}{V}\sum_{\mathbf{k}\sigma}\left(-\frac{\partial n(\mathbf{k})}{\partial\varepsilon_0(\mathbf{k})}\right)\frac{mv_\alpha^2(\mathbf{k})}{\omega+\lambda^2 M(\mathbf{k},\mathbf{q},\omega)} \quad (32)$$

to second order in λ. Finally, summations over $\mathbf{k}$ and $i\omega_n$ give the first two terms in the generalized Drude conductivity formula

$$\sigma_{\alpha\alpha}(\omega) = \frac{ie^2 n_{\alpha\alpha}}{m[\omega+\lambda^2 M_\alpha(\omega)]}. \quad (33)$$

In Eqs. (32) and (33), $v_\alpha(\mathbf{k}) = (1/e)J_\alpha(\mathbf{k},\mathbf{k})$ is the electron group velocity and

$$n_{\alpha\alpha}(\mathbf{q}) = \frac{1}{V}\sum_{\mathbf{k}\sigma}\frac{m}{e^2}|J_\alpha(\mathbf{k},\mathbf{k}_+)|^2\frac{n(\mathbf{k})-n(\mathbf{k}_+)}{\varepsilon_0(\mathbf{k}_+)-\varepsilon_0(\mathbf{k})}$$

$$\approx \frac{1}{V}\sum_{\mathbf{k}\sigma}mv_\alpha^2(\mathbf{k})\left(-\frac{\partial n(\mathbf{k})}{\partial\varepsilon_0(\mathbf{k})}\right) \quad (34)$$

is the effective number of charge carriers, with $n_{\alpha\alpha} = n_{\alpha\alpha}(\mathbf{q}\approx\mathbf{0})$. Finally, $n(\mathbf{k})$ is the momentum-distribution function from Eq. (21).

D. Current-current correlation function

The comparison of the analytically continued forms of Eqs. (26)–(28) for $\mu=\alpha$ and $\nu=\bar{\alpha}$ with the second Kubo formula [12]

$$\sigma_{\alpha\alpha}(\mathbf{q},\omega) = \frac{i}{\omega}\left(\frac{e^2 n_{\alpha\alpha}(\mathbf{q})}{m}+\pi_{\alpha\alpha}(\mathbf{q},\omega)\right) \quad (35)$$

shows that the first term in the expansion (26) is nothing but the exact expression for the diamagnetic conductivity. Therefore the second contribution in Eq. (26) in this case can be understood as the first term in the expansion of the current-current correlation function $\pi_{\alpha\alpha}(\mathbf{q},iv_n)$ in powers of λ^2. Therefore the current-current correlation function $\pi_{\alpha\alpha}(\mathbf{q},iv_n)$ from Eq. (29) can also be shown as

$$\pi_{\alpha\alpha}(\mathbf{q},iv_n) = \frac{1}{V}\sum_{\mathbf{k}\sigma}|J_\alpha(\mathbf{k},\mathbf{k}_+)|^2$$

$$\times\frac{1}{\beta\hbar}\sum_{i\omega_n}\frac{\mathcal{G}(\mathbf{k},i\omega_{n+})-\mathcal{G}(\mathbf{k}_+,i\omega_{n+})}{\varepsilon_0(\mathbf{k}_+,\mathbf{k})}$$

$$\times\frac{-\lambda^2\Delta\Pi(\mathbf{k},\mathbf{q},iv_n,i\omega_n)}{i\hbar v_n+\varepsilon(\mathbf{k},\mathbf{k}_+)+\lambda^2\Delta\Pi(\mathbf{k},\mathbf{q},iv_n,i\omega_n)}. \quad (36)$$

The expressions (29) and (36) show thus the current-current correlation function $\pi_{\alpha\alpha}(\mathbf{q},iv_n)$ in terms of the indirect and direct contributions, respectively. These expressions can be combined with any of three conductivity formulas mentioned above.

The expression (36) for the current-current correlation function is the second important result of the present paper. It shows that it is possible to determine the structure of $\pi_{\alpha\alpha}(\mathbf{q},iv_n)$ by using the same methods as that used to calculate $\pi_{00}(\mathbf{q},iv_n)$. As pointed out in Sec. VII, this can be very useful in those *ab initio* calculations in which the damping energy $\hbar\Sigma^i(\mathbf{k},\omega)$ in the momentum distribution function $n(\mathbf{k})$ is approximated by η [where $n(\mathbf{k})\approx f(\mathbf{k})$].

V. WEAK ELECTRON-PHONON INTERACTIONS

It is instructive first to determine the Boltzmann spectral representation of the conductivity tensor from the previous section for $H'=H_1'$, the case which is of primary interest in graphene for frequencies $\omega\approx\omega_{\mathrm{LO}\mathbf{q}'}$. We combine the iterative solution of the quantum transport equation (24) with the electron-hole self-energy conductivity formula (31), and then show the $\mathbf{k}$- and ω-dependent memory function $M(\mathbf{k},\mathbf{q},\omega)\approx M_\alpha(\mathbf{k},\omega)$ and the ω-dependent memory function $M_\alpha(\omega)$ from Eqs. (32) and (33) in terms of the electron-hole self-energy $\Delta\Pi(\mathbf{k},\mathbf{q},\omega,\varepsilon)\approx\Delta\Pi_\alpha(\mathbf{k},\omega,\varepsilon)$. For simplicity, we consider the case of longitudinal external fields, where $\sigma_{\alpha\alpha}(\mathbf{q},\omega)$ is described in terms of the direct contributions.

A. Boltzmann representation of $\sigma_{\alpha\alpha}(\mathbf{q},\omega)$

After inserting the spectral representation of the propagators $\mathcal{G}(\mathbf{k},i\omega_n)$ and $\mathcal{D}_\nu(\mathbf{q}',iv_m)$, Eqs. (12) and (13), into Eqs. (26)–(28), we obtain the Boltzmann representation of the electron-hole self-energy conductivity formula:

$$\sigma_{\alpha\alpha}(\mathbf{q},\omega)$$

$$= \frac{1}{V}\sum_{\mathbf{k}\sigma}|J_\alpha(\mathbf{k},\mathbf{k}_+)|^2\int_{-\infty}^\infty\frac{d\varepsilon}{2\pi}\frac{[\mathcal{A}(\mathbf{k},\varepsilon)-\mathcal{A}(\mathbf{k}_+,\varepsilon)]f(\varepsilon)}{\varepsilon(\mathbf{k}_+,\mathbf{k})}$$

$$\times\frac{i\hbar}{\hbar\omega+\varepsilon(\mathbf{k},\mathbf{k}_+)+i\eta}\left(1-\lambda^2\frac{\hbar\Delta\Pi_\alpha(\mathbf{k},\omega,\varepsilon)}{\hbar\omega+\varepsilon(\mathbf{k},\mathbf{k}_+)}+\cdots\right)$$

$$= \frac{i\hbar e^2}{m}\frac{1}{V}\sum_{\mathbf{k}\sigma}\int_{-\infty}^\infty\frac{d\varepsilon}{2\pi}\frac{[\mathcal{A}(\mathbf{k},\varepsilon)-\mathcal{A}(\mathbf{k}_+,\varepsilon)]f(\varepsilon)}{\varepsilon(\mathbf{k}_+,\mathbf{k})}$$

$$\times\frac{mv_\alpha^2(\mathbf{k})}{\hbar\omega+\varepsilon(\mathbf{k},\mathbf{k}_+)+\lambda^2\hbar\Delta\Pi_\alpha(\mathbf{k},\omega,\varepsilon)}, \quad (37)$$

with $\hbar\omega\gg\varepsilon(\mathbf{k},\mathbf{k}_+)$. In the leading approximation, the electron-hole self-energy is given by $\Delta\Pi_\alpha(\mathbf{k},\omega,\varepsilon)\approx\Delta\Pi_\alpha^{(AB)}(\mathbf{k},\omega,\varepsilon)$, where

$$\hbar\Delta\Pi_\alpha^{(AB)}(\mathbf{k},\omega,\varepsilon)$$

$$= -\frac{1}{N}\sum_{\nu\mathbf{k}'}\left(1-\frac{v_\alpha(\mathbf{k}')}{v_\alpha(\mathbf{k})}\right)|G_\nu(\mathbf{k},\mathbf{k}')|^2$$

$$\times\int_{-\infty}^\infty\frac{d\varepsilon'}{2\pi}\int_{-\infty}^\infty\frac{d\omega'}{2\pi}\mathcal{A}(\mathbf{k}',\varepsilon')\mathcal{B}_\nu(\mathbf{k}'-\mathbf{k},\omega')$$

$$\times\sum_{s=\pm 1}\frac{f^b(\omega')+f(s\varepsilon')}{\hbar\omega+i\eta+s(\varepsilon-\varepsilon')+\hbar\omega'}. \quad (38)$$
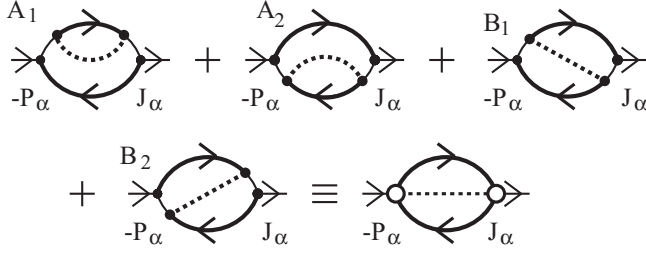
FIG. 5. The diagrammatic illustration of the λ^2 contribution to $\sigma_{\alpha\alpha}(\mathbf{q},\omega)$ from Eqs. (37), (26), and (28).

Figure 5 illustrates the λ^2 contribution to $\sigma_{\alpha\alpha}(\mathbf{q},\omega)$ in this case. The indices A and B stand, respectively, for the A and B RPA-

like series of diagrams for $\mathcal{F}(\mathbf{k},\mathbf{k}',iv_m)$ in the single-electron self-energy and in the vertex corrections term.

B. k- and ω-dependent memory function

In weakly interacting systems, the factor $\int (d\varepsilon/2\pi)[\mathcal{A}(\mathbf{k},\varepsilon) - \mathcal{A}(\mathbf{k}_+,\varepsilon)]f(\varepsilon)$ in Eq. (37) can be approximated by $n(\mathbf{k}) - n(\mathbf{k}_+)$, with ε replaced by $\varepsilon(\mathbf{k})$. In this way, we obtain the memory function

$$M_\alpha(\mathbf{k},\omega) \approx M_\alpha^{(AB)}(\mathbf{k},\omega) = \Delta\Pi_\alpha^{(AB)}(\mathbf{k},\omega,\varepsilon(\mathbf{k})), \quad (39)$$

and Eq. (37) reduces to the memory-function conductivity formula (32).

It should be noticed that the result of the direct diagrammatic calculation of the $(H_1')^2$ contributions to the memory function $M_\alpha(\mathbf{k},\omega)$,

$$\hbar M_\alpha^{[2]}(\mathbf{k},\omega) = -\frac{1}{N}\sum_{\nu\mathbf{k}'}\left(1 - \frac{v_\alpha(\mathbf{k}')}{v_\alpha(\mathbf{k})}\right)|G_\nu(\mathbf{k},\mathbf{k}')|^2 \sum_{s=\pm 1}\sum_{s'=\pm 1}\frac{s'[f^b(s'\omega_{\nu\mathbf{k}'-\mathbf{k}}) + f(s\varepsilon(\mathbf{k}'))]}{\hbar\omega + i\eta + s\varepsilon(\mathbf{k},\mathbf{k}') + s'\hbar\omega_{\nu\mathbf{k}'-\mathbf{k}}}, \quad (40)$$

can be obtained by substituting the expressions (15) into Eq. (38). Figure 6 shows $\sigma_{\alpha\alpha}^{(2)}(\omega)$ in this case. Notice again that $s'[f^b(s'\omega_{\nu\mathbf{k}'-\mathbf{k}}) + f(s\varepsilon(\mathbf{k}'))] = f^b(\omega_{\nu\mathbf{k}'-\mathbf{k}}) + f(s'\varepsilon(\mathbf{k}'))$. Consequently, the memory function (40) for the states at the Fermi surface can be shown in the form

$$\hbar M_\alpha^{[2]}(\mathbf{k}_F,\omega) = -\sum_{s=\pm 1}s\frac{1}{N}\sum_{\nu\mathbf{k}'}\left(1 - \frac{v_\alpha(\mathbf{k}')}{v_\alpha(\mathbf{k}_F)}\right)|G_\nu(\mathbf{k}_F,\mathbf{k}')|^2 \sum_{s'=\pm 1}\frac{f^b(\omega_{\nu\mathbf{k}'-\mathbf{k}_F}) + f(s'\varepsilon(\mathbf{k}'))}{s(\hbar\omega + i\eta) + \varepsilon(\mathbf{k}_F,\mathbf{k}') + s'\hbar\omega_{\nu\mathbf{k}'-\mathbf{k}_F}}$$

$$\equiv -\hbar\widetilde{\Sigma}^{[2]}(\mathbf{k}_F,\omega + i\eta) + \hbar\widetilde{\Sigma}^{[2]}(\mathbf{k}_F, -\omega - i\eta), \quad (41)$$

where $\widetilde{\Sigma}^{[2]}(\mathbf{k},\omega + i\eta)$ is given by Eq. (14) with $|G_\nu(\mathbf{k},\mathbf{k}')|^2$ replaced by $|\widetilde{G}_\nu(\mathbf{k},\mathbf{k}')|^2 \equiv [1 - v_\alpha(\mathbf{k}')/v_\alpha(\mathbf{k})]|G_\nu(\mathbf{k},\mathbf{k}')|^2$. A similar relation holds between the electron-hole self-energy $\Delta\Pi_\alpha^{(AB)}(\mathbf{k},\omega,\varepsilon)$ from Eq. (38) and $\Sigma(\mathbf{k},\omega)$ from Eq. (11). For a further analysis of the dynamical conductivity in Sec. VII, it is useful also to introduce the auxiliary spectral function $\widetilde{\mathcal{A}}(\mathbf{k},\varepsilon)$ which is defined by Eq. (20) with $\Sigma(\mathbf{k},\omega)$ replaced by $\widetilde{\Sigma}(\mathbf{k},\omega)$.

C. ω-dependent memory function

The frequency-dependent memory function $M_\alpha(\omega)$ is a complex relaxation function in the hydrodynamic transport equations [12,13,35]. In order to avoid Mori's projection operator technique to determine its structure, Götze and Wölfle developed a slightly different method which is called here the common memory-function method [36]. The resulting memory function is closely related to the relaxation rate $\hbar/\tau_{tr}$ calculated by using the variational method [37]. In this

approach, the conductivity tensor is given by the generalized Drude formula (33).

The memory-function conductivity formula (32) leads to the same expression for $\sigma_{\alpha\alpha}(\omega)$, provided that $M_\alpha(\mathbf{k},\omega)$ is replaced with its average over the Fermi surface,

$$M_\alpha(\omega) = \frac{1}{n_{\alpha\alpha}}\frac{1}{V}\sum_{\mathbf{k}\sigma}mv_\alpha^2(\mathbf{k})\left(-\frac{\partial n(\mathbf{k})}{\partial\varepsilon(\mathbf{k})}\right)M_\alpha(\mathbf{k},\omega). \quad (42)$$

In weakly interacting systems with nearly isotropic Fermi surfaces, we can also write

$$M_\alpha(\omega) \approx M_\alpha(\mathbf{k}_F,\omega), \quad (43)$$

in the leading approximation. $M_\alpha(\omega)$ can be defined in a slightly different way by using the Drude form of $\sigma_{\alpha\alpha}(\omega)$, Eq. (44). In this case, $M_\alpha(\omega)$ represents the average of $M_\alpha(\mathbf{k},\omega)$ over all occupied states.

D. Drude representation of $\sigma_{\alpha\alpha}(\mathbf{q},\omega)$

When the self-energy $\Delta\Pi(\mathbf{k},\mathbf{q},\omega,\varepsilon)$ depends on the direction of $\mathbf{q} = q_\alpha\hat{e}_\alpha$, but not on its magnitude [$\approx \Delta\Pi_\alpha(\mathbf{k},\omega,\varepsilon)$], then we can change the dummy variables in Eq. (37) in a way explained in Appendix B. The resulting conductivity formula represents the Drude representation of Eq. (37), and, together with Eq. (38), is the third important result of the present
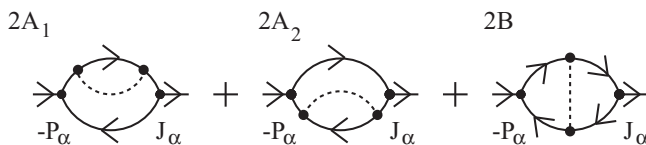

FIG. 6. Three $(H_1')^2$ contributions to $\sigma_{\alpha\alpha}^{(2)}(\omega)$, labeled by $2A_1$ (electron self-energy term), $2A_2$ (hole self-energy term), and $2B = 2B_1 + 2B_2$ (vertex correction).

paper:

$$\sigma_{\alpha\alpha}(\omega) \approx \frac{ie^2}{m}\frac{1}{V}\sum_{\mathbf{k}\sigma}\gamma_{\alpha\alpha}(\mathbf{k})\int_{-\infty}^{\infty}\frac{d\varepsilon}{2\pi}\frac{\mathcal{A}(\mathbf{k},\varepsilon)f(\varepsilon)}{\omega + \Delta\Pi_{\alpha}(\mathbf{k},\omega,\varepsilon)}. \quad (44)$$

Here, $\gamma_{\alpha\alpha}(\mathbf{k}) = (m/\hbar^2)\partial^2\varepsilon_0(\mathbf{k})/\partial k_\alpha^2$ is the dimensionless reciprocal effective mass tensor.

The expression (44) is characterized by two different damping energies. The first one, $\Sigma^i(\mathbf{k},\omega)$ in $\mathcal{A}(\mathbf{k},\varepsilon)$, describes the width of the quasiparticle peak in the single-electron spectral function, while the second one, $\Pi^i_\alpha(\mathbf{k},\omega,\varepsilon)$, gives the description of the relaxation processes in a way which is consistent with the law of conservation of energy.

The factor $[1 - v_\alpha(\mathbf{k}')/v_\alpha(\mathbf{k})]$ in Eqs. (38) and (40) is of critical importance in understanding the electrical conductivity. It makes the damping energy $\Pi^i_\alpha(\mathbf{k},\omega,\varepsilon)$ different from $\Sigma^i(\mathbf{k},\omega) - \Sigma^i(\mathbf{k}_+,\omega_+)$. It is responsible for the complete cancellation of the contributions to $\Pi_\alpha(\mathbf{k},\omega,\varepsilon)$ originating from the $\mathbf{q}' \approx \mathbf{0}$ scattering processes. It is found to be useful for studying temperature dependencies of the electrical and the thermal conductivity at low temperatures as well [38]. Most importantly, it describes the way in which the singular $\mathbf{q}' \approx \mathbf{0}$ long-range Coulomb interactions drop out of the transport equations [39]. Similarly, the factor $1/[\hbar\omega + i\eta + s(\varepsilon - \varepsilon') + \hbar\omega']$ takes care of the law of conservation of energy. Evidently, in the memory-function conductivity formula, as well as in the relaxation-time approximation, this law is satisfied only on average [because ε in Eq. (38) is replaced by $\varepsilon(\mathbf{k})$ in this case].

It is straightforward to generalize the discussion of the expressions (38) and (44) to cover strongly interacting electronic systems as well, but only if the quasiparticle pole in $\mathcal{A}(\mathbf{k},\varepsilon)$ is clearly distinguished from the rest of this spectral function. In this case, $n(\mathbf{k})$ is associated with the coherent part of $\mathcal{A}(\mathbf{k},\varepsilon)$ and can be approximated by $n^{\mathrm{coh}}(\mathbf{k})/\alpha(\mathbf{k})$, with $n^{\mathrm{coh}}(\mathbf{k}) \approx f(\mathbf{k})$, where $\alpha(\mathbf{k})$ is the corresponding reduction factor usually related to strong Mott correlations. Such formalism proves useful in studies of the normal state $\omega \approx 0$ properties of underdoped cuprates [11].

VI. RESIDUAL CONTRIBUTIONS

It is apparent that the expression (38) for the electron-hole self-energy is incomplete, even in the weakly interacting $H' = H'_1$ case. The simplest way to see this is to consider weak nonretarded interactions ($H' = H'_2$) and compare the result with the textbook expression for the $(H'_2)^2$ contributions to $\hbar/\tau_{\mathrm{tr}}$ [37–39].

For $H' = H'_2$, low-order perturbation theory for the memory function $M_\alpha(\mathbf{k},\omega)$ starts with the $(H'_2)^2$ contributions, because the $(H'_2)^1$ diagrams from Fig. 6 are already included in $\Delta\varepsilon^{\mathrm{HF}}(\mathbf{k})$, and then, together with $\varepsilon_0(\mathbf{k})$, neglected in the $\omega^2 \gg q_\alpha^2 v_\alpha^2(\mathbf{k})$ limit. The set of four mutually related irreducible $(H'_2)^2$ contributions to $\sigma_{\alpha\alpha}^{(2)}(\omega)$ is shown in Fig. 7. The first two contributions are the $2A_1$ and $2B_1$ diagrams from Fig. 5 in which $[|G_\nu(\mathbf{k},\mathbf{k}')|^2/N\hbar]\mathcal{D}_\nu(\mathbf{q}',\omega)$ is replaced by $[|\varphi(\mathbf{q}')|^2/V]\widetilde{\chi}(\mathbf{q}',\omega)$. The $4C_1$ and $4D_1$ diagrams represent a similar pair of contributions, which is missing in Fig. 5, and which is characterized by the factor $[v_\alpha(\mathbf{k}'_+)/v_\alpha(\mathbf{k}) - v_\alpha(\mathbf{k}')/v_\alpha(\mathbf{k})]$. When put together, these four diagrams result
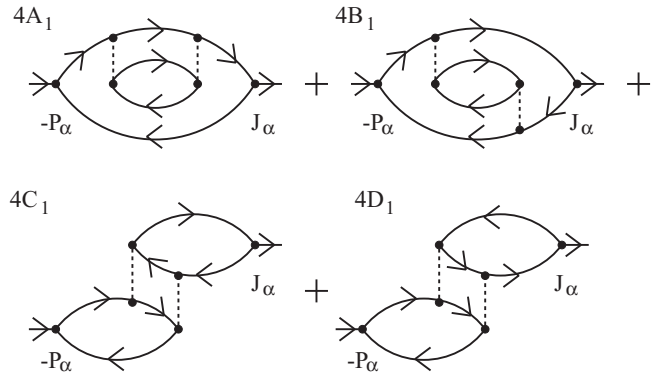

FIG. 7. The first set of four mutually related contributions to $\sigma_{\alpha\alpha}^{(2)}(\omega)$ that are proportional to $(H'_2)^2$ [or $(H'_1)^4$].

in the factor $[v_\alpha(\mathbf{k}) + v_\alpha(\mathbf{k}'_+) - v_\alpha(\mathbf{k}') - v_\alpha(\mathbf{k}_+)]$ in

$$\hbar M_\alpha^{[4]}(\mathbf{k},\omega) = -\sum_{\mathbf{k}'\mathbf{q}'\sigma'}\frac{|\varphi(\mathbf{q}')|^2}{V^2}\frac{1}{v_\alpha(\mathbf{k})}[v_\alpha(\mathbf{k}) + v_\alpha(\mathbf{k}'_+)$$
$$- v_\alpha(\mathbf{k}') - v_\alpha(\mathbf{k}_+)][f(\varepsilon(\mathbf{k}')) - f(\varepsilon(\mathbf{k}'_+))]$$
$$\times \sum_{s=\pm 1}\frac{f^b(\omega(\mathbf{k}'_+,\mathbf{k}')) + f(\varepsilon(\mathbf{k}_+))}{\hbar\omega + i\eta + s\varepsilon(\mathbf{k},\mathbf{k}') + s\varepsilon(\mathbf{k}'_+,\mathbf{k}_+)}$$

$$(45)$$

[similarly for $\Delta\Pi_\alpha^{[4]}(\mathbf{k},\omega,\varepsilon)$]. This factor is responsible not only for the complete cancellation of the $\mathbf{q}' \approx \mathbf{0}$ forward scattering processes, but also for a strong reduction of the intensity of the normal backward scattering processes. Therefore, in the absence of the scattering processes described by H'_1, the resistivity of weakly interacting electronic systems comes predominantly from the umklapp backward scattering processes by other electrons. This is of particular importance in the two-dimensional systems because the number of thermally activated intraband plasmons is proportional to $f^b(\omega_{\mathrm{pl}}(\mathbf{q}')) \approx k_B T/\hbar\omega_{\mathrm{pl}}(\mathbf{q}')$, leading to significant temperature effects in $\Sigma^i(\mathbf{k},\omega)$ and to less pronounced effects in $\Pi^i_\alpha(\mathbf{k},\omega,\varepsilon)$.

A straightforward calculation gives similar expressions for $M_\alpha^{[4]}(\mathbf{k},\omega)$ and $\Delta\Pi_\alpha^{[4]}(\mathbf{k},\omega,\varepsilon)$ associated with the $(H'_1)^4$ diagrams in Fig. 7. The $4A_1$ and $4B_1$ contributions are already included in Eq. (38), while the $4C_1$ and $4D_1$ contributions represent the leading corrections. To calculate the latter contributions, we must recognize the contributions in the quantum transport equation (24) which are directly related to the $4C_1$ and $4D_1$ diagrams, and recollect all diagrams in the C and D series in a way illustrated in Fig. 8. The final result

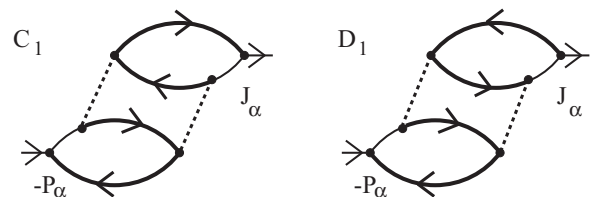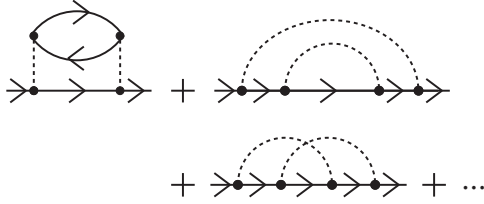FIG. 8. The diagrammatic illustration of the $\Delta\Pi_\alpha^{(CD)}(\mathbf{k},\omega,\varepsilon)$ contributions to $\sigma_{\alpha\alpha}^{(2)}(\omega)$.

FIG. 9. The first three $(H_1')^4$ contributions to $\Sigma^{[4]}(\mathbf{k},\omega)$.

for the electron-hole self-energy is the expression

$$\Delta\Pi_\alpha(\mathbf{k},\omega,\varepsilon) \approx \Delta\Pi_\alpha^{(AB)}(\mathbf{k},\omega,\varepsilon) + \Delta\Pi_\alpha^{(CD)}(\mathbf{k},\omega,\varepsilon). \quad (46)$$

Equations (46) and (38), together with the expression for $\Delta\Pi_\alpha^{(CD)}(\mathbf{k},\omega,\varepsilon)$, represent the result of high-order perturbation theory for the electron-hole self-energy in weakly interacting systems with $H' = H_1'$.

There are two similar sets of irreducible $(H_1')^4$ diagrams in $\sigma_{\alpha\alpha}^{(2)}(\omega)$. The first one is associated with the third diagram in Fig. 9. This set is usually called the crossing diagrams. These diagrams play an important role in standard theory of the Anderson weak localization, but they are disregarded in the present discussion of the relaxation processes. The second set includes the second diagram in Fig. 9 and the corresponding vertex corrections. These contributions are incorporated in the present self-consistent Hartree-Fock scheme in the usual way, through the renormalized single-electron Green's function and the reducible four-point interaction.

VII. COMPARISON WITH OTHER WORK

The variational treatment of the transport coefficients [37] and the common memory-function method [36] are just two widely used methods that are closely related to the electron-hole self-energy conductivity formula (44). There is a rich variety of similar conductivity formulas which are usually used in the *ab initio* calculations. They can be divided into two groups. The first group, corresponding to the case in which $\Sigma^i(\mathbf{k},\omega) \to \eta$ and $\Pi_\alpha^i(\mathbf{k},\omega,\varepsilon) \to \Gamma$ [23], was briefly discussed in Ref. [12]. Let us now examine in some detail the second group, which is characterized by $\Pi_\alpha(\mathbf{k},i\nu_n,i\omega_n) \to \Sigma(\mathbf{k},i\omega_n) - \Sigma(\mathbf{k}_+,i\omega_{n+})$, corresponding to the second Kubo formula for $\sigma_{\alpha\alpha}(\mathbf{q},\omega)$ with the vertex effects neglected. The latter approach is most frequently encountered in the study of strongly interacting low-dimensional electronic systems [15]. It has been used in early studies of $\sigma_{\alpha\alpha}(\omega)$ in graphene as well [16,17].

A. Naive treatment of vertex effects

The difficulty of getting solution to the self-consistent equation for the renormalized intraband current vertex function usually leads to neglecting the vertex corrections in the second Kubo formula for $\sigma_{\alpha\alpha}(\mathbf{q},\omega)$. In such approaches, the emphasis is usually on the detailed numerical calculations of the spectral function $\mathcal{A}(\mathbf{k},\varepsilon)$, rather than on the general requirements, related, for example, to the charge continuity equation or the Ward identity. The principal problem here is that the resulting conductivity formulas overestimate the role of the scattering from acoustic phonons [38] and, in the two-dimensional

systems, of the scattering from intraband plasmon modes. The resulting conductivity formulas have serious deficiencies, in the first place, in describing the temperature effects in the low-frequency conductivity.

Nevertheless, we can use a similar idea to simplify the conductivity formulas (37) and (44) by replacing $\mathcal{A}(\mathbf{k},\varepsilon)$ with $\widetilde{\mathcal{A}}(\mathbf{k},\varepsilon)$. In this way, we obtain much simpler expressions for $\sigma_{\alpha\alpha}(\mathbf{q},\omega)$ with again only one damping function, $\widetilde{\Sigma}^i(\mathbf{k},\omega)$. However, the conductivity formulas obtained in this way treat local charge conservation in the system satisfactorily, and they are expected to give reasonable results in the usual Fermi liquid regime (low temperatures and $\hbar\omega \to 0$).

An alternative to the use of Eq. (44), with $\mathcal{A}(\mathbf{k},\varepsilon)$ replaced by $\widetilde{\mathcal{A}}(\mathbf{k},\varepsilon)$, is the approach based on Eqs. (31) and (8) with $\mathcal{G}(\mathbf{k},i\omega_n) \to \widetilde{\mathcal{G}}(\mathbf{k},i\omega_n)$ and $\Delta\Pi_\alpha(\mathbf{k},\omega,\varepsilon) \to \Delta\widetilde{\Pi}_\alpha^0(\mathbf{k},\omega,\varepsilon)$. The result is

$$\sigma_{\alpha\alpha}(\mathbf{q},\omega) = \frac{i\hbar e^2}{m}\frac{1}{V}\sum_{\mathbf{k}\sigma}mv_\alpha^2(\mathbf{k})\int_{-\infty}^\infty\frac{d\varepsilon}{2\pi}\int_{-\infty}^\infty\frac{d\varepsilon'}{2\pi}$$
$$\times\frac{\widetilde{\mathcal{A}}(\mathbf{k},\varepsilon)\widetilde{\mathcal{A}}(\mathbf{k}_+,\varepsilon')}{\varepsilon(\mathbf{k}_+,\mathbf{k})}\frac{f(\varepsilon)-f(\varepsilon')}{\hbar\omega+i\eta+\varepsilon-\varepsilon'}. \quad (47)$$

The real part of this function can be approximated by

$$\mathrm{Re}\{\sigma_{\alpha\alpha}(\omega)\} = \hbar e^2\frac{1}{V}\sum_{\mathbf{k}\sigma}v_\alpha^2(\mathbf{k})\int_{-\infty}^\infty\frac{d\varepsilon}{2\pi}\frac{1}{2}\widetilde{\mathcal{A}}(\mathbf{k},\varepsilon)\widetilde{\mathcal{A}}(\mathbf{k},\varepsilon+\hbar\omega)$$
$$\times\frac{f(\varepsilon)-f(\varepsilon+\hbar\omega)}{\hbar\omega}. \quad (48)$$

The well-known result for the real part of the dynamical conductivity, obtained by using the second Kubo formula for $\sigma_{\alpha\alpha}(\omega)$ with the vertex corrections neglected [14], corresponds to Eq. (48), with $\widetilde{\mathcal{A}}(\mathbf{k},\varepsilon)\widetilde{\mathcal{A}}(\mathbf{k},\varepsilon+\hbar\omega)$ replaced by $\mathcal{A}(\mathbf{k},\varepsilon)\mathcal{A}(\mathbf{k},\varepsilon+\hbar\omega)$. This means that the conclusions of the *ab initio* studies of the dynamical conductivity in strongly interacting systems based on the second Kubo formula can be made more convincing if the complete cancellation of the $\mathbf{q} \approx \mathbf{0}$ forward scattering processes and a significant reduction of the normal backward scattering processes discussed above are taken into account by the redefinition of the coupling functions $|G_\nu(\mathbf{k},\mathbf{k}')|^2$ and $|\varphi(\mathbf{q})|^2$ in the single-electron self-energy $\Sigma(\mathbf{k},i\omega_n)$ in a way suggested by Eqs. (40) and (45).

B. Relation to Fermi liquids

The most important difference between the present approach and the common form of the second Kubo formula is their relation to the Landau-Silin transport equations and to the resulting expression for the conductivity tensor [40]. The simplest way to see this difference is to recall the corresponding expressions for the current-current correlation function. In the first case, $\pi_{\alpha\alpha}(\mathbf{q},\omega)$ is described in terms of the direct contributions, Eq. (36), and, as a result, we obtain the memory-function conductivity formula simply by replacing $\Delta\Pi_\alpha(\mathbf{k},\omega,\varepsilon)$ by $M_\alpha(\mathbf{k},\omega)$. The standard Fermi liquid result corresponds to the replacements $M_\alpha(\mathbf{k},\omega) \to M_\alpha(\omega) \to i/\tau_{\mathrm{tr}}$ [39]. Therefore here we have the one-to-one correspondence of the conductivity formulas (37) and (44) with the standard transport theory. On the other hand, in the second case,

$\pi_{\alpha\alpha}(\mathbf{q},\omega)$ is shown in terms of the indirect processes in Eq. (29) and the idea to simplify the corresponding expression for $\sigma_{\alpha\alpha}(\mathbf{q},\omega)$ by $\Delta\Pi_{\alpha}(\mathbf{k},\omega,\varepsilon) \to M_{\alpha}(\mathbf{k},\omega)$ does not work here. In simple electronic systems, the second approach gives indeed the same result as the standard transport theory, but there is no direct correspondence between the two procedures [14].

C. Elementary excitations

One important consequence of this one-to-one correspondence is that the structure of the λ^2 term in Eq. (44) can help us to identify all elementary excitations which participate in the damping effects in the conductivity tensor (and in other response functions). In the Landau damping regime, the damping is associated with the creation of one electron-hole pair such that $\hbar\omega \approx \varepsilon(\mathbf{k}_+,\mathbf{k})$. The processes included in Eq. (38) correspond to the creation of one electron-hole pair plus one phonon, resulting in $\hbar\omega \approx \varepsilon(\mathbf{k}',\mathbf{k}) \pm \hbar\omega_{\nu\mathbf{q}'}$. The processes shown in Fig. 7 illustrate the creation of two electron-hole pairs with $\hbar\omega \approx \varepsilon(\mathbf{k}',\mathbf{k}) + \varepsilon(\mathbf{k}_+,\mathbf{k}'_+)$. Finally, higher order corrections to $\Delta\Pi_{\alpha}(\mathbf{k},\omega,\varepsilon)$ are expected to produce more complicated real excitations in the system. The intraband plasmon modes are just an example.

VIII. DAMPING OF DIRAC PLASMONS

At the level of approximation used in Sec. III D, the memory function $M_{\alpha}^{\mathrm{op}}(\mathbf{k}_F,\omega)$ from Eq. (41) is largely unaffected by vertex corrections. The expressions (37) and (44) for the conductivity tensor can be simplified now by replacing $\Pi_{\alpha}(\mathbf{k},\omega,\varepsilon)$ by $M_{\alpha}(\omega)$ and $\Sigma^i(\mathbf{k},\omega)$ by η, where $M_{\alpha}(\omega) \approx M_{\alpha}^{\mathrm{op}}(\mathbf{k}_F,\omega) + \delta M_{\alpha}(\omega)$,

$$M_{\alpha}^{\mathrm{op}}(\mathbf{k}_F,\omega) = \widetilde{\Sigma}^{\mathrm{op}}(\mathbf{k}_F,-\omega-i\eta) - \widetilde{\Sigma}^{\mathrm{op}}(\mathbf{k}_F,\omega+i\eta), \quad (49)$$

and $\delta M_{\alpha}^i(\omega) = \tilde{a} + |\hbar\omega|\tilde{b}$, resulting in the generalized Drude formula

$$\sigma_{\alpha\alpha}^{\mathrm{intra}}(\omega) \approx \sigma_{\alpha\alpha}^{dc} \frac{\left[\omega + M_{\alpha}^r(\omega) - iM_{\alpha}^i(\omega)\right]iM_{\alpha}^i(0)}{\left[\omega + M_{\alpha}^r(\omega)\right]^2 + \left[M_{\alpha}^i(\omega)\right]^2}. \quad (50)$$

In this section, the index intra is explicitly written, for clarity.

The real and imaginary parts of $M_{\alpha}^{\mathrm{op}}(\mathbf{k}_F,\omega)$ are shown in Fig. 10. Notice that the memory function possesses particle-hole symmetry, i.e., $M_{\alpha}^r(-\omega) = -M_{\alpha}^r(\omega)$ and $M_{\alpha}^i(-\omega)\} = M_{\alpha}^i(\omega)$, in agreement with the analytical properties of the response function $\sigma_{\alpha\alpha}^{\mathrm{intra}}(\omega)$. It is also interesting to notice that the corresponding contribution to the band mass enhancement factor $m_{\alpha}^b(\omega)/m = [1 + \lambda_{\alpha}(\omega)]$ at $\omega = 0$ is $\lambda_{\alpha}^{\mathrm{op}}(\omega = 0) \approx 0.38$ [here $\lambda_{\alpha}(\omega) = M_{\alpha}^r(\omega)/\omega = \lambda_{\alpha}^{\mathrm{op}}(\omega) + \delta\lambda_{\alpha}(\omega)$]. Consequently, the effective number of charge carriers $n_{\alpha\alpha}^{\mathrm{eff}}$ and the damping energy Γ_{α} in the ordinary Drude formula

$$\sigma_{\alpha\alpha}^{\mathrm{intra}}(\omega) \approx \frac{ie^2 n_{\alpha\alpha}^{\mathrm{eff}}}{m(\omega + i\Gamma_{\alpha})}, \quad (51)$$

which is a reasonable approximation for $\sigma_{\alpha\alpha}^{\mathrm{intra}}(\omega)$ from Eq. (50) for energies $\hbar\omega \ll \hbar M_{\alpha}^i(0)$, are $n_{\alpha\alpha}^{\mathrm{eff}} = n_{\alpha\alpha}^{\mathrm{intra}}/[1 + \lambda_{\alpha}(0)]$ and $\Gamma_{\alpha} = M_{\alpha}^i(0)/[1 + \lambda_{\alpha}(0)]$.

The function $\mathrm{Re}\{\sigma_{\alpha\alpha}^{\mathrm{intra}}(\mathbf{q},\omega)\}/\sigma_{\alpha\alpha}^{dc}$ is illustrated in Fig. 11 for $\mathbf{q} \approx 0$. Here, $\sigma_{\alpha\alpha}^{dc} = [e^2 n_{\alpha\alpha}^{\mathrm{intra}}/m M_{\alpha}^i(0)] = (e^2 n_{\alpha\alpha}^{\mathrm{eff}}/m\Gamma_{\alpha})$ is the dc conductivity in the generalized Drude model. The figure illustrates the transfer of the conductivity spectral weight over
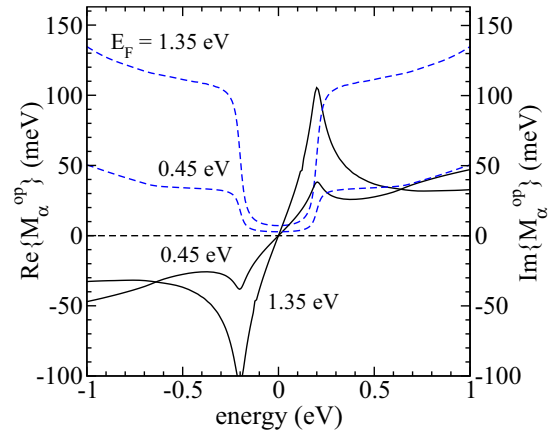

FIG. 10. (Color online) The real part (solid lines) and the imaginary part (dashed lines) of the memory function $M_{\alpha}^{\mathrm{op}}(\mathbf{k}_F,\omega)$, Eq. (49), for $t = 2.52$ eV, $E_F = 0.45, 1.35$ eV, $|\widetilde{G}_{\mathrm{op}}|^2 = 0.2$ eV^2, $\hbar\omega_{\mathrm{op}} = 0.2$ eV, $\eta = \hbar\Sigma^i = 20$ meV, and $T = 30$ K. Here, $\mathrm{Re}\{M_{\alpha}^{\mathrm{op}}(\mathbf{k}_F,0)\} = 0$.

the relevant energy scale $\hbar\omega_{\mathrm{LO}\mathbf{q}'}$ with increasing the electron-phonon coupling constant [16,17]. The result is typical of the weakly interacting electron-phonon systems. The main frequency-dependent effects in $\sigma_{\alpha\alpha}(\mathbf{q},\omega)$ for frequencies $\omega \approx \omega_{\mathrm{LO}\mathbf{q}'}$ are thus related to the four processes from Fig. 5 in which one electron-hole pair is created in combination with one in-plane optical phonon. A more realistic description of the dynamical conductivity at $\omega \approx \omega_{\mathrm{LO}\mathbf{q}'}$ follows after using realistic phonon dispersions, the $\mathbf{k}$-dependent electron-phonon coupling functions, and the $\mathbf{k}$-dependent memory function. The main effect is the suppression of the maximum in Fig. 11 at $\omega \approx \omega_{\mathrm{op}}$ and a more precise description of the high-energy conductivity.

We can use this form of the memory function $M_{\alpha}(\omega)$ to describe the dependence on frequency of the position and
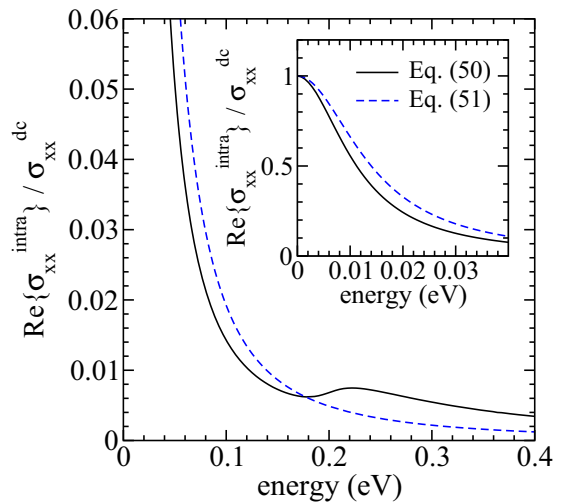

FIG. 11. (Color online) Solid line: the real part of the intraband conductivity (50) for $E_F = 0.45$ eV. The parameters are the same as in Fig. 10, with $\delta M_{\alpha}^i(\omega) = \tilde{a} + |\hbar\omega|\tilde{b}$ and $\tilde{a} = 0.01$ eV, $\tilde{b} = 0.015$. Dashed line: the result of the relaxation-time approximation, Eq. (51), for $\hbar\Gamma_{\alpha} = 14$ meV.

the shape of the intraband plasmon peak in the energy loss function $-\text{Im}\{1/\varepsilon(\mathbf{q},\omega)\}$ as well. In the heavily doped case with $\hbar\omega < E_F$, the effects of the interband electron-hole excitations are small [12,23] and their contribution to the longitudinal dielectric function $\varepsilon(\mathbf{q},\omega)$ can be approximated by a real constant $\tilde{\varepsilon}_\infty$. In this case, we can write

$$\varepsilon(\mathbf{q},\omega) \approx \tilde{\varepsilon}_\infty - \frac{2\pi q}{\omega^2}\left(\frac{e^2}{m}n_{\alpha\alpha}^{\text{intra}}(\mathbf{q}) + \pi_{\alpha\alpha}^{\text{intra}}(\mathbf{q},\omega)\right) \quad (52)$$

(here, $\mathbf{q} = q_\alpha\hat{e}_\alpha$ again). The inverse of $\varepsilon(\mathbf{q},\omega)$ is given by

$$\frac{1}{\varepsilon(\mathbf{q},\omega)} = \frac{\omega^2/\tilde{\varepsilon}_\infty}{\omega^2 - \omega_{\text{pl}}^2(\mathbf{q},\omega) + i\omega\Gamma_{\text{pl}}(\mathbf{q},\omega)}, \quad (53)$$

where

$$\omega_{\text{pl}}^2(\mathbf{q},\omega) \approx \omega\frac{2\pi q}{\tilde{\varepsilon}_\infty}\text{Im}\big[\sigma_{\alpha\alpha}^{\text{intra}}(\mathbf{q},\omega)\big]$$

$$= \frac{2\pi q}{\tilde{\varepsilon}_\infty}\left(\frac{e^2}{m}n_{\alpha\alpha}^{\text{intra}}(\mathbf{q}) + \text{Re}\big[\pi_{\alpha\alpha}^{\text{intra}}(\mathbf{q},\omega)\big]\right)$$

$$\equiv \big[\omega_{\text{pl}}^0(\mathbf{q})\big]^2 + \Delta\omega_{\text{pl}}^2(\mathbf{q},\omega),$$

$$\omega\Gamma_{\text{pl}}(\mathbf{q},\omega) \approx \omega\frac{2\pi q}{\tilde{\varepsilon}_\infty}\text{Re}\big[\sigma_{\alpha\alpha}^{\text{intra}}(\mathbf{q},\omega)\big] = -\frac{2\pi q}{\tilde{\varepsilon}_\infty}\text{Im}\big[\pi_{\alpha\alpha}^{\text{intra}}(\mathbf{q},\omega)\big].$$

$$(54)$$

Equations (53) and (54) show that, for frequencies $\omega \approx \omega_{\text{pl}}^0(\mathbf{q})$, the function $-\text{Im}[1/\varepsilon(\mathbf{q},\omega)]$ can be understood as a typical boson spectral function in which the frequency $\omega_{\text{pl}}^0(\mathbf{q})$ plays the role of the bare boson frequency and $\pi_{\alpha\alpha}^{\text{intra}}(\mathbf{q},\omega)$ is the corresponding self-energy. In the relaxation-time approximation studied in Ref. [12], there is no dramatic change of the shape of the intraband plasmon peak for $\omega_{\text{pl}}(\mathbf{q}) \approx \omega_{\text{LO}\mathbf{q}'}$. In the generalized Drude model (50), on the other hand, the change in the shape of this peak reflects the steplike increase
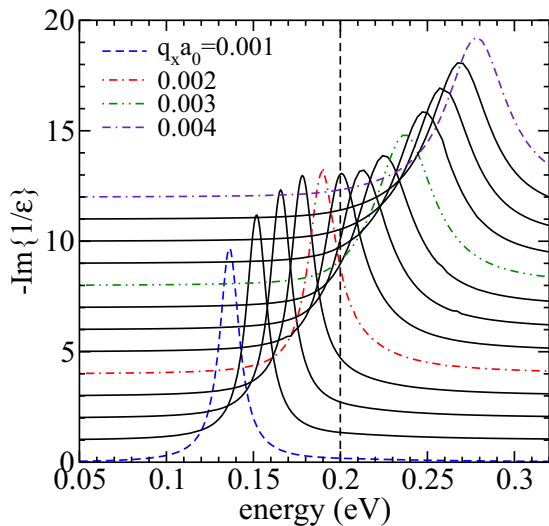

FIG. 12. (Color online) The energy loss function $-\text{Im}\{1/\varepsilon(\mathbf{q},\omega)\}$ as a function of the wave vector $\mathbf{q} = (q_x,0)$, for $q_x a_0 = 0.001$, $E_F = 0.4$ eV, $\tilde{\varepsilon}_\infty = 1$, and for $\hbar\omega$ close to the energy of the in-plane optical phonons. The conductivity is given by Eq. (50). The parameters are the same as in Fig. 11. The wave vector q_x increases with the step $\Delta q_x a_0 = 0.00025$ up to $q_x a_0 = 0.004$. a_0 is the Bohr radius.

of $\text{Im}\{M_\alpha^{\text{op}}(\omega)\}$ from Fig. 10 at $\hbar\omega \approx \omega_{\text{op}}$. Figure 12 shows the dependence of $-\text{Im}\{1/\varepsilon(\mathbf{q},\omega)\}$ on $\mathbf{q}$, for $E_F = 0.4$ eV. The result is characterized by the increase in full width at half maximum from the value ≈ 20 meV below the energy $\hbar\omega_{\text{op}} = 0.2$ eV to the value ≈ 30 meV above this energy. This is in reasonably good agreement with experiment [7]. We defer a detailed discussion of the effects illustrated in Figs. 10–12 to Ref. [10].

IX. CONCLUSION

In this work, we have derived the longitudinal dynamical conductivity tensor in a general weakly interacting electron-phonon system. Starting with the general form of the self-consistent Bethe-Salpeter equations for the auxiliary electron-hole propagators, we have formulated perturbation theory for calculating the longitudinal conductivity tensor in powers of the completely irreducible four-point interaction. In this way, we determine the Boltzmann and the Drude spectral representations of the dynamical conductivity in weakly interacting electron-phonon systems and find the structure of the corresponding electron-hole self-energy. We have explained the relation between the electron-hole self-energy and the ω- and $\mathbf{k}$-dependent memory function, and rederived the general Drude conductivity formula.

The results are applied to heavily doped graphene, which is the prototype of weakly interacting single-band electron-phonon systems. We have calculated the single-electron spectral function for $E_F = 1.35$ eV, the dynamical conductivity for $E_F = 0.45$ eV, and the energy loss function for $E_F = 0.4$ eV in a model in which the scattering by in-plane optical phonons is treated in the leading approximation and all other scattering channels are taken into account phenomenologically. The results are found to be in good agreement with experiment. The explicit treatment of the interband scattering processes in the intraband channel and a detailed description of the interband conductivity will be given in a future presentation [10].

ACKNOWLEDGMENTS

APPENDIX A: COUPLING TO IN-PLANE OPTICAL PHONONS AND TO ELECTROMAGNETIC FIELDS IN GRAPHENE

In simple electronic systems with covalent bonding the conduction electrons couple to phonon modes through the variation of the amplitude of bond energies [41]. Similarly, the coupling to the external vector potential is described by a gauge-invariant tight-binding minimal substitution, i.e., through the variation of the phase of the same bond energies [34].

In graphene, these two coupling Hamiltonians, together with the bare electronic Hamiltonian H_0^{el}, can be obtained by
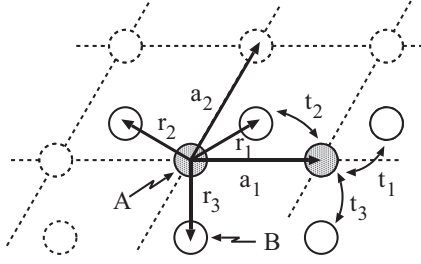
FIG. 13. The relevant vectors in the honeycomb lattice in graphene. The $t_j \equiv \tilde{t}(\bar{\mathbf{R}}, \mathbf{r}_j)$ represent three hopping integrals between neighboring $2p_z$ orbitals. Two different carbon sites in the unit cell are labeled by A and B.

replacing the bond energy $t(\bar{\mathbf{R}}, \mathbf{r}_j)$ in H_0^{el} by

$$\tilde{t}(\bar{\mathbf{R}}, \mathbf{r}_j) = [t + \delta t(\bar{\mathbf{R}}, \mathbf{r}_j)]e^{i\Phi(\bar{\mathbf{R}}, \mathbf{r}_j)} \qquad (A1)$$

($\bar{\mathbf{R}} = \mathbf{R}_n + \mathbf{r}_j/2$ is the position of the bond in question and the $\mathbf{r}_j$ are the relative positions of three first neighbors, as shown in Fig. 13). We can write now

$$\widetilde{H}_0^{\text{el}} = -\sum_{n\sigma} \sum_{j=1}^3 [\tilde{t}(\bar{\mathbf{R}}, \mathbf{r}_j)c_{Bnj\sigma}^\dagger c_{An\sigma} + \text{H.c.}]$$

$$\equiv -\sum_{\mathbf{R}\boldsymbol{\delta}\sigma} [\tilde{t}_{\mathbf{R}+\boldsymbol{\delta}\mathbf{R}} b_\sigma^\dagger(\mathbf{R} + \boldsymbol{\delta})a_\sigma(\mathbf{R}) + \text{H.c.}]$$

$$\approx H_0^{\text{el}} + H_1' + H_1^{\text{ext}} + H_2^{\text{ext}}, \qquad (A2)$$

with [12,20,21,42]

$$\delta t(\bar{\mathbf{R}}, \mathbf{r}_j) = \frac{\partial t(\bar{\mathbf{R}}, \mathbf{r}_j)}{\partial \mathbf{r}_j} \cdot (\mathbf{u}_{\nu n j}^B - \mathbf{u}_{\nu n}^A),$$

$$\Phi(\bar{\mathbf{R}}, \mathbf{r}_j) = \frac{e}{\hbar c} \mathbf{r}_j \cdot \mathbf{A}^{\text{ext}}(\bar{\mathbf{R}}). \qquad (A3)$$

The operator $c_{An\sigma}^\dagger$ creates an electron at the site A at the position $\mathbf{R}_n$ and $c_{Bnj\sigma}^\dagger$ creates an electron at the site B at the position $\mathbf{R}_n + \mathbf{r}_j$. The expression in the second row of Eq. (A2) represents the standard notation for $\widetilde{H}_0^{\text{el}}$ [9,16].

In the representation of the delocalized orbitals $\{l\mathbf{k}\}$ the four terms in Eq. (A2) can be shown in the following forms:

$$H_0^{\text{el}} = \sum_{ll'} \sum_{\mathbf{k}\sigma} H_0^{l'l}(\mathbf{k})c_{l'\mathbf{k}\sigma}^\dagger c_{l\mathbf{k}\sigma},$$

$$H_1' = \sum_{\nu\mathbf{q}} \frac{g_\nu}{\sqrt{N}} u_{\nu\mathbf{q}} \sum_{ll'} \sum_{\mathbf{k}\sigma} q_\nu^{l'l}(\mathbf{k}_+,\mathbf{k})c_{l'\mathbf{k}+\mathbf{q}\sigma}^\dagger c_{l\mathbf{k}\sigma},$$

$$H_1^{\text{ext}} = -\frac{1}{c} \sum_{\mathbf{q}\alpha} A_\alpha^{\text{ext}}(\mathbf{q}) \sum_{ll'} \sum_{\mathbf{k}\sigma} J_\alpha^{l'l}(\mathbf{k}_+,\mathbf{k})c_{l'\mathbf{k}+\mathbf{q}'\sigma}^\dagger c_{l\mathbf{k}\sigma},$$

$$H_2^{\text{ext}} = \frac{e^2}{2mc^2} \sum_{\mathbf{q}\mathbf{q}'\alpha\beta} A_\alpha^{\text{ext}}(\mathbf{q} - \mathbf{q}')A_\beta^{\text{ext}}(\mathbf{q}')$$

$$\times \sum_{ll'} \sum_{\mathbf{k}\sigma} \gamma_{\alpha\beta}^{l'l}(\mathbf{k}_+,\mathbf{k}; 2)c_{l'\mathbf{k}+\mathbf{q}'\sigma}^\dagger c_{l\mathbf{k}\sigma}, \qquad (A4)$$

with $u_{\nu\mathbf{q}} = u_{\nu\mathbf{q}}^A = -u_{\nu\mathbf{q}}^B$ and $u_{\nu\mathbf{q}} = u_{\nu\mathbf{q}}^A = u_{\nu\mathbf{q}}^B$ for the optical and acoustic phonons, respectively, and $g_\nu = \partial t/\partial r_j$. As usual,

the index $l = A, B$ labels two different $2p_z$ orbitals on two carbon sites in the unit cell.

In the common nearest-neighbor tight-binding approximation, with the overlap parameter s set equal to zero, the matrix elements in Eqs. (A4) are given by the well-known expressions

$$H_0^{BA}(\mathbf{k}) = t(\mathbf{k}) = -t \sum_{j=1}^3 e^{-i\mathbf{k}\cdot\mathbf{r}_j}, \qquad (A5)$$

and

$$q_\nu^{BA}(\mathbf{k}_+,\mathbf{k}) = -\frac{1}{a_{\text{CC}}} \sum_{j=1}^3 \mathbf{e}_\mathbf{q}^\nu \cdot \mathbf{r}_j\, e^{-i(\mathbf{k}+\mathbf{q}/2)\cdot\mathbf{r}_j}$$

$$\times \frac{1}{u_{\nu\mathbf{q}}} \left(u_{\nu\mathbf{q}}^A e^{-i\mathbf{q}\cdot\mathbf{r}_j/2} - u_{\nu\mathbf{q}}^B e^{i\mathbf{q}\cdot\mathbf{r}_j/2}\right),$$

$$J_\alpha^{BA}(\mathbf{k}_+,\mathbf{k}) = \frac{ite}{\hbar} \sum_{j=1}^3 r_{j\alpha} e^{-i(\mathbf{k}+\mathbf{q}/2)\cdot\mathbf{r}_j} = \frac{e}{\hbar} \frac{\partial t(\mathbf{k} + \mathbf{q}/2)}{\partial k_\alpha},$$

$$\gamma_{\alpha\beta}^{BA}(\mathbf{k}_+,\mathbf{k}; 2) = \frac{mt}{\hbar^2} \sum_{j=1}^3 r_{j\alpha}r_{j\beta} e^{-i(\mathbf{k}+\mathbf{q}/2)\cdot\mathbf{r}_j} = \frac{m}{\hbar^2} \frac{\partial^2 t(\mathbf{k}+\mathbf{q}/2)}{\partial k_\alpha \partial k_\beta}. \qquad (A6)$$

The change to the diagonal $\{s\mathbf{k}\}$ representation is straightforward. For example, the bare electron dispersions in Eq. (2) in the main text are $\varepsilon_{\pi^*,\pi}^0(\mathbf{k}) + \mu = \pm|t(\mathbf{k})|$ with

$$|t(\mathbf{k})| = \pm t\sqrt{3 + 2\cos k_x a + 4\cos \frac{k_x a}{2} \cos \frac{\sqrt{3}k_y a}{2}}. \quad (A7)$$

Similarly, the intraband electron-phonon coupling functions and the intra- and interband current vertices are given, respectively, by

$$G_\nu^{ss}(\mathbf{k}',\mathbf{k}) = \sqrt{\left(\hbar g_\nu^2/2M_\nu\omega_{\nu\mathbf{q}'}\right)} q_\nu^{ss}(\mathbf{k}',\mathbf{k}),$$

$$q_\nu^{ss}(\mathbf{k}',\mathbf{k}) = \sum_{ll'} q_\nu^{l'l}(\mathbf{k}',\mathbf{k})U_{\mathbf{k}'}(l',s)U_\mathbf{k}^*(l,s), \qquad (A8)$$

and

$$J_\alpha^{ss'}(\mathbf{k}',\mathbf{k}) = \sum_{ll'} J_\alpha^{l'l}(\mathbf{k}',\mathbf{k})\, U_{\mathbf{k}'}(l',s)U_\mathbf{k}^*(l,s'), \qquad (A9)$$

with $s,s' \in \{\pi,\pi^*\}$. The transformation matrix elements $U_\mathbf{k}(l,s)$ are given by [9,12]

$$\begin{pmatrix} U_\mathbf{k}(A,\pi^*) & U_\mathbf{k}(A,\pi) \\ U_\mathbf{k}(B,\pi^*) & U_\mathbf{k}(B,\pi) \end{pmatrix} = \frac{1}{\sqrt{2}} \begin{pmatrix} 1 & 1 \\ e^{-i\theta_\mathbf{k}} & -e^{-i\theta_\mathbf{k}} \end{pmatrix}. \quad (A10)$$

The auxiliary phase $\theta_\mathbf{k}$ is defined by $\tan\theta_\mathbf{k} = t_i(\mathbf{k})/t_r(\mathbf{k})$, with $t_r(\mathbf{k})$ and $t_i(\mathbf{k})$ being the real and the imaginary parts of $t(\mathbf{k})$.

APPENDIX B: ELECTRON-HOLE SELF-ENERGY APPROXIMATION

After simple algebraic manipulations with Eq. (24), which include the interchange of variables $\mathbf{k}\, i\omega_n \rightleftharpoons \mathbf{k}'\, i\omega_m$ in the last term on the right-hand side of the equation, we obtain the

integral equation for $\Phi_{\tilde{\alpha}}^0(\mathbf{k},\mathbf{k}_+,i\omega_n,i\omega_{n+})$ of the form

$$\sum_{\mathbf{k}\sigma} J_\alpha(\mathbf{k},\mathbf{k}_+) \sum_{i\omega_n} \Phi_{\tilde{\alpha}}^0(\mathbf{k},\mathbf{k}_+,i\omega_n,i\omega_{n+})$$

$$= \sum_{\mathbf{k}\sigma} \sum_{i\omega_n} \left\{ \frac{\mathcal{G}(\mathbf{k}_+,i\omega_{n+}) - \mathcal{G}(\mathbf{k},i\omega_n)}{\hbar[i\hbar\nu_n + \varepsilon(\mathbf{k},\mathbf{k}_+)]} J_\alpha(\mathbf{k},\mathbf{k}_+) P_\alpha(\mathbf{k}_+,\mathbf{k}) \right.$$

$$- \left[J_\alpha(\mathbf{k},\mathbf{k}_+) \frac{\hbar\Delta\Sigma(\mathbf{k},i\omega_n) - \hbar\Delta\Sigma(\mathbf{k}_+,i\omega_{n+})}{i\hbar\nu_n + \varepsilon(\mathbf{k},\mathbf{k}_+)} \right.$$

$$+ \sum_{\mathbf{k}'\sigma'} J_\alpha(\mathbf{k}',\mathbf{k}'_+) \frac{1}{\beta\hbar} \sum_{i\omega_m} \frac{\mathcal{G}(\mathbf{k}',i\omega_m) - \mathcal{G}(\mathbf{k}'_+,i\omega_{m+})}{i\hbar\nu_n + \varepsilon(\mathbf{k}',\mathbf{k}'_+)}$$

$$\left. \times \Delta U(\mathbf{k}'_+,\mathbf{k},\mathbf{k}_+,\mathbf{k}',i\omega_{m+},i\omega_n,i\omega_{n+},i\omega_m) \right]$$

$$\left. \times \Phi_{\tilde{\alpha}}^0(\mathbf{k},\mathbf{k}_+,i\omega_n,i\omega_{n+}) \right\}. \tag{B1}$$

It is easily seen that the simplest form of $\Phi_{\tilde{\alpha}}^0(\mathbf{k},\mathbf{k}_+,i\omega_n,i\omega_{n+})$ that satisfies this integral equation is the solution of the ordinary self-consistent equation

$$[i\hbar\nu_n + \varepsilon(\mathbf{k},\mathbf{k}_+) + \hbar\Delta\Pi(\mathbf{k},\mathbf{k}_+,i\omega_n,i\omega_{n+})]$$

$$\times \Phi_{\tilde{\alpha}}^0(\mathbf{k},\mathbf{k}_+,i\omega_n,i\omega_{n+})$$

$$\approx \frac{1}{\hbar}[\mathcal{G}(\mathbf{k}_+,i\omega_{n+}) - \mathcal{G}(\mathbf{k},i\omega_n)] P_\alpha(\mathbf{k}_+,\mathbf{k}), \tag{B2}$$

where

$$\hbar\Delta\Pi(\mathbf{k},\mathbf{k}_+,i\omega_n,i\omega_{n+})$$

$$\approx \hbar\Delta\Sigma(\mathbf{k},i\omega_n) - \hbar\Delta\Sigma(\mathbf{k}_+,i\omega_{n+})$$

$$+ \sum_{\mathbf{k}'\sigma'} \frac{1}{\beta\hbar} \sum_{i\omega_m} [\mathcal{G}(\mathbf{k}',i\omega_m) - \mathcal{G}(\mathbf{k}'_+,i\omega_{m+})] \frac{J_\alpha(\mathbf{k}',\mathbf{k}'_+)}{J_\alpha(\mathbf{k},\mathbf{k}_+)}$$

$$\times \Delta U(\mathbf{k}'_+,\mathbf{k},\mathbf{k}_+,\mathbf{k}',i\omega_{m+},i\omega_n,i\omega_{n+},i\omega_m) \tag{B3}$$

represents the retarded part of the intraband electron-hole self-energy.

We now insert $J_\alpha(\mathbf{k},\mathbf{k}_+) \approx ev_\alpha(\mathbf{k})$ and $-P_\alpha(\mathbf{k}_+,\mathbf{k}) \approx p_\alpha(-\mathbf{q})$ in the expression for $\pi_{\alpha\tilde{\alpha}}(\mathbf{q},i\nu_n)$, Eq. (23), where $v_\alpha(\mathbf{k}) = (1/\hbar)\partial\varepsilon^0(\mathbf{k})/\partial k_\alpha$ is again the bare electron group velocity and $p_\alpha(-\mathbf{q}) = ie/q_\alpha$ is the intraband dipole vertex function, and set $\varepsilon(\mathbf{k},\mathbf{k}_+)$ in the denominator equal to zero. The result is

$$\sigma_{\alpha\alpha}(\mathbf{q},i\nu_n) = \frac{1}{V} \sum_{\mathbf{k}\sigma} \frac{1}{\beta\hbar} \sum_{i\omega_n} \frac{ev_\alpha(\mathbf{k})p_\alpha(-\mathbf{q})}{i\hbar\nu_n + \hbar\Delta\Pi(\mathbf{k},\mathbf{k}_+,i\omega_n,i\omega_{n+})}$$

$$\times [\mathcal{G}(\mathbf{k},i\omega_n) - \mathcal{G}(\mathbf{k}_+,i\omega_{n+})]. \tag{B4}$$

Finally, after using the replacement $\mathbf{k} + \mathbf{q} \to \mathbf{k}$ in the second term, we obtain

$$\sigma_{\alpha\alpha}(\mathbf{q},i\nu_n) \approx \frac{1}{V} \sum_{\mathbf{k}\sigma} \frac{1}{\beta\hbar} \sum_{i\omega_n} e[v_\alpha(\mathbf{k}) - v_\alpha(\mathbf{k}-\mathbf{q})]$$

$$\times p_\alpha(-\mathbf{q}) \frac{\mathcal{G}(\mathbf{k},i\omega_n)}{i\hbar\nu_n + \hbar\Delta\Pi(\mathbf{k},\mathbf{k}_+,i\omega_n,i\omega_{n+})}, \tag{B5}$$

with

$$e[v_\alpha(\mathbf{k}) - v_\alpha(\mathbf{k}-\mathbf{q})]p_\alpha(-\mathbf{q}) \approx \frac{ie^2}{\hbar} \frac{\partial^2\varepsilon^0(\mathbf{k})}{\partial k_\alpha^2} = \frac{ie^2\hbar}{m}\gamma_{\alpha\alpha}(\mathbf{k}). \tag{B6}$$

Equations (B4) and (B5) are the electron-hole self-energy expressions for the intraband conductivity tensor $\sigma_{\alpha\alpha}(\mathbf{q},i\nu_n)$. The former one represents the Boltzmann representation of $\sigma_{\alpha\alpha}(\mathbf{q},i\nu_n)$ and the latter one the Drude representation. In the case in which the dependence of $\Delta\Pi(\mathbf{k},\mathbf{k}_+,i\omega_n,i\omega_{n+})$ on the internal frequency $i\omega_n$ can be simplified in the way explained in Sec. V B, the analytically continued form of the expression (B4) reduces to the memory-function conductivity formula (32). The expressions (37) and (44) represent, respectively, the spectral representations of the expressions (B4) and (B5).

---

[1] K. S. Novoselov, A. K. Geim, S. V. Morozov, D. Jiang, M. I. Katsnelson, I. V. Grigorieva, S. V. Dubonos, and A. A. Firsov, Nature (London) **438**, 197 (2005).

[2] Y. Zhang, Y.-W. Tan, H. L. Stormer, and P. Kim, Nature (London) **438**, 201 (2005).

[3] Z. Q. Li, E. A. Henriksen, Z. Jiang, Z. Hao, M. C. Martin, P. Kim, H. L. Stormer, and D. N. Basov, Nat. Phys. **4**, 532 (2008).

[4] A. Bostwick, T. Ohta, T. Seyller, K. Horn, and E. Rotenberg, Nat. Phys. **3**, 36 (2007).

[5] I. Pletikosić, M. Kralj, M. Milun, and P. Pervan, Phys. Rev. B **85**, 155447 (2012).

[6] T. Eberlein, U. Bangert, R. R. Nair, R. Jones, M. Gass, A. L. Bleloch, K. S. Novoselov, A. Geim, and P. R. Briddon, Phys. Rev. B **77**, 233406 (2008).

[7] H. Yan, T. Low, W. Zhu, Y. Wu, M. Freitag, X. Li, F. Guinea, P. Avoutis, and F. Xia, Nat. Photon. **7**, 394 (2013).

[8] K. Ziegler, Phys. Rev. Lett. **97**, 266802 (2006).

[9] A. H. Castro Neto, F. Guinea, N. M. R. Peres, K. S. Novoselov, and A. K. Geim, Rev. Mod. Phys. **81**, 109 (2009).

[10] Z. Rukelj and I. Kupčić (unpublished).

[11] I. Kupčić and I. Jedovnicki (unpublished).

[12] I. Kupčić, Phys. Rev. B **90**, 205426 (2014).

[13] R. Kubo, M. Toda, and N. Hashitsume, *Statistical Physics II* (Springer-Verlag, Berlin, 1995).

[14] G. D. Mahan, *Many-particle Physics* (Plenum Press, New York, 1990).

[15] M. J. Rozenberg, G. Kotliar, and H. Kajueter, Phys. Rev. B **54**, 8452 (1996).

[16] N. M. R. Peres, T. Stauber, and A. H. Castro Neto, Europhys. Lett. **84**, 38002 (2008).

[17] J. P. Carbotte, E. J. Nicol, and S. G. Sharapov, Phys. Rev. B **81**, 045419 (2010).

[18] I. Kupčić, Z. Rukelj, and S. Barišić, J. Phys. Condens. Matter **25**, 145602 (2013).

[19] A. C. Ferrari, J. C. Meyer, V. Scardaci, C. Casiraghi, M. Lazzeri, F. Mauri, S. Piscanec, D. Jiang, K. S. Novoselov, S. Roth, and A. K. Geim, Phys. Rev. Lett. **97**, 187401 (2006).

[20] D. M. Basko, New J. Phys. **11**, 095011 (2009).

[21] I. Kupčić, J. Raman Spectrosc. **43**, 1 (2012).

[22] M. Jablan, H. Buljan, and M. Soljačić, Phys. Rev. B **80**, 245435 (2009).

[23] V. Despoja, D. Novko, K. Dekanić, M. Šunjić, and L. Marušić, Phys. Rev. B **87**, 075447 (2013).

[24] S. Reich, J. Maultzsch, C. Thomsen, and P. Ordejón, Phys. Rev. B **66**, 035412 (2002).

[25] A. A. Abrikosov, L. P. Gorkov, and I. E. Dzyaloshinski, *Methods of Quantum Field Theory in Statistical Physics* (Dover, New York, 1975).

[26] I. E. Dzyaloshinskii and A. I. Larkin, Zh. Eksp. Teor. Fiz. **65**, 411 (1973) [Sov. Phys. JETP **38**, 202 (1974)].

[27] J. Solyom, Adv. Phys. **28**, 201 (1979).

[28] D. Vollhardt and P. Wölfle, Phys. Rev. B **22**, 4666 (1980).

[29] A. L. Fetter and J. D. Walecka, *Quantum Theory of Many-Particle Systems* (McGraw–Hill, London, 1971).

[30] J. R. Schrieffer, *Theory of Superconductivity* (Benjamin, New York, 1964).

[31] I. Kupčić, Z. Rukelj, and S. Barišić, J. Phys. Condens. Matter **26**, 195601 (2014).

[32] N. A. Sinitsyn, J. E. Hill, H. Min, J. Sinova, and A. H. MacDonald, Phys. Rev. Lett. **97**, 106804 (2006).

[33] N. A. Sinitsyn, A. H. MacDonald, T. Jungwirth, V. K. Dugaev, and J. Sinova, Phys. Rev. B **75**, 045315 (2007).

[34] I. Kupčić and S. Barišić, Phys. Rev. B **75**, 094508 (2007).

[35] D. Forster, *Hydrodynamic Fluctuations, Broken Symmetry, and Correlation Functions* (Benjamin, London, 1975).

[36] W. Götze and P. Wölfle, Phys. Rev. B **6**, 1226 (1972).

[37] J. M. Ziman, *Electrons and Phonons* (Oxford University Press, London, 1972).

[38] A. A. Abrikosov, *Fundamentals of the Theory of Metals* (Nort-Holland, Amsterdam, 1988).

[39] D. Pines and P. Noziéres, *The Theory of Quantum Liquids I* (Addison-Wesley, New York, 1989).

[40] P. M. Platzman and P. A. Wolff, *Waves and Interactions in Solid State Plasmas* (Academic Press, New York, 1973).

[41] S. Barišić, Phys. Rev. B **5**, 932 (1972).

[42] T. Ando, J. Phys. Soc. Jpn. **75**, 124701 (2006).